



This is to certify that the

thesis entitled

FABRICATION OF AEROGEL - DERIVED SILICA/SILICON CARBIDE COMPOSITES

presented by

Chittoor K. Mohanakrishnan

has been accepted towards fulfillment of the requirements for

M.S. degree in Chemical Engr.

Lenns J. Miller Major professor

Date____8-8-90

O-7639

MSU is an Affirmative Action/Equal Opportunity Institution



PLACE IN RETURN BOX to remove this checkout from your record. TO AVOID FINES return on or before date due.

400€	DATE DUE	DATE DUE
DEC 0 9		
·		

MSU Is An Affirmative Action/Equal Opportunity Institution chairc\databus.pm3-p.1

FABRICATION OF AEROGEL - DERIVED SILICA/SILICON CARBIDE COMPOSITES

Вy

Chittoor K. Mohanakrishnan

A THESIS

Submitted to

Michigan State University
in partial fulfillment of the requirements
for the degree of

MASTER OF SCIENCE

Department of Chemical Engineering

ABSTRACT

FABRICATION OF AEROGEL - DERIVED SILICA/SILICON CARBIDE COMPOSITES

Βv

Chittoor K. Mohanakrishnan

A new process to fabricate ceramic composites has been developed using the sol-gel approach. The matrix of the composite is gel-derived silica and the second phase of the material system is polycarbosilane-derived SiC. Silica gel prepared by a sol-gel process was dried using supercritical CO₂ to produce a porous silica gel matrix. The porous matrix was partially densified by a thermal treatment and was infiltrated with a solution of polycarbosilane in hexane. The infiltrated matrix was then densified by a high temperature anneal to form the composite.

Composite specimens of reasonable densities were fabricated in different geometries. The maximum amount of polycarbosilane that could be infiltrated in the matrix was 12 % by weight of gel. Higher polycarbosilane contents resulted in extensive macroscopic cracking of the specimen. The variation of density and microhardness of the composite as a function of polycarbosilane content was determined.



ACKNOWLEDGEMENTS

The author wishes to thank Dr. Dennis J. Miller for his guidance and support throughout the course of the project; Dr. C.T. Lira, for his suggestions and comments; Dr. E. Case, for allowing the use of his high temperature furnace; Mr. Bharath Rangarajan, for tirelessly making gels; and Mr. C.-C. Chiu for conducting mechanical tests on the materials.

TABLE OF CONTENTS

LIST	OF TABLESviii
LIST	OF FIGURES
1. IN	TRODUCTION
	1.1 General Introduction
	1.2 Sol-gel routes to ceramic materials
	1.2.1 Formation of gels: sol to gel conversion 3
	1.2.2 Drying of gels: supercritical drying 7
	1.2.3 Densification of gels: gel to ceramic
	conversion8
	1.3 Polymer pyrolysis routes to ceramic materials
	1.4 Ceramic composites
	1.4.1 Types of Ceramic Matrix Composites 14
	1.4.2 Mechanisms of toughening in CMCs
	1.4.3 Processing and fabrication of Ceramic
	Matrix Composites
	1.4.3.1 Conventional techniques
	1.4.3.2 Sol-gel techniques

2. MATERIALS AND METHODS
2.1 Starting materials
2.1.1 Silica aerogels:preparation and
characterization
2.1.2 Polycarbosilane: characterization 28
2.2 Processing method
2.2.1 Pre-densification of silica aerogels
2.2.2 Polycarbosilane infiltration
2.2.3 Cross-linking of polycarbosilane 32
2.2.4 Pyrolysis of polycarbosilane and
densification of the silica aerogel matrix 33
2.3 High temperature muffle tube furnace
2.4 Characterization of the composite

3. RESULTS AND DISCUSSION

3.1 Results of initial experiments on silica	
aerogels and polycarbosilane	. (
3.1.1 Initial experiments on silica aerogels	. (
3.1.1.1 Mercury porosimetry of silica	
aerogels4	. (
3.1.1.2 Nitrogen adsorption on silica	
aerogels4	. 1
3.1.1.3 Behaviour of silica aerogels	
upon thermal treatment-TGA	
and FTIR studies	.]
3.1.2 Initial experiments on polycarbosilane 5	1
3.1.2.1 Solubility of PCS in hexane 5	1
3.1.2.2 Behaviour of PCS upon thermal	
treatment-TGA and FTIR	
studies	1
3.2 Results of pre-densification of silica aerogels 5	8
3.3 Results of polycarbosilane infiltration	2
3.4 Results of cross-linking of polycarbosilane 6	4
3.5 Results of the pyrolysis of polycarbosilane and	
densification of silica	5
CONCLUSIONS AND RECOMMENDATIONS	2
LIST OF REFERENCES	5
APPENDIX A 8	(

LIST OF TABLES

1.	Examples of commercially available ceramic fibers 16
2.	Polycarbosilane solubility information
3.	Variation of density of silica aerogel with
	hold time
4.	Variation of density of silica aerogel with
	storage time
5.	Variation of density of silica aerogel
	with temperature
6.	Polycarbosilane infiltration data
7.	Conditions for cross-linking of polycarbosilane
	infiltrated in silica aerogel matrix
A1.	Pore size distribution of silica aerogel by
	mercury porosimetry

LIST OF FIGURES

1.	Structure of silica aerogel (from Ref. 61) 30
2.	Work tube assembly
3.	Seal assembly
4.	Inert gas flow arrangement
5.	BET adsorption isotherm of silica aerogel
6.	TGA curve of silica aerogel
7.	FTIR spectrum of silica aerogel
8.	FTIR spectrum of silica aerogel heated to 1250°C (dense silica)
9.	FTIR spectrum of silica aerogel heated to 150°C 47
10.	FTIR spectrum of silica aerogel heated to 450°C 48
11.	FTIR spectrum of silica aerogel heated to 600°C 49
12.	FTIR spectrum of silica aerogel heated to 1050°C 50
13.	TGA curve of cross-linked polycarbosilane (PCS) 52
14.	FTIR spectrum of cross-linked polycarbosilane (PCS) 54
15.	FTIR spectrum of cross-linked PCS heated to 500°C
16.	FTIR spectrum of cross-linked PCS heated to 650°C
17.	FTIR spectrum of cross-linked PCS heated to 800°C 57
18.	Variation of density of processed specimens
	with anneal temperature
19.	FTIR spectrum of SiO ₂ /SiC composite 69
20.	Photograph of processed specimens: top-silica aerogel, middle-densified silica, and
	bottom-SiO ₂ /SiC composite

Chapter 1 INTRODUCTION

1.1 GENERAL INTRODUCTION

Ceramics have long been used as high temperature materials, for a variety of applications. Ceramics can be broadly classified as oxide and non-oxide based materials. Silica (including silicates), alumina, magnesia, and zirconia all belong to the oxide category and represent the largest fraction of structural ceramics. Other than being a high temperature material, ceramics are useful because of their low densities, low thermal conductivities, and in some cases, good electrical properties. However, all these materials are limited in use under very high-stress, high temperature applications. For example, silicates form viscous liquids that creep; magnesia has a large

thermal expansion coefficient, and zirconia and alumina suffer from poor thermal shock properties. Under these severe conditions, it has been found that certain non-oxide materials like carbides, borides and nitrides showed better properties. Most important among these materials are silicon carbide and silicon nitride. They have high strength at high temperatures, excellent thermal shock resistance, and low thermal expansions.

The concept of using ceramics to fabricate composite materials emerged in the 1960's and has since been widely studied. A composite material is made up of a bulk matrix phase, a second minor phase, and the interface between the two phases. The choice of the two phases depends on the end properties desired. Ceramic composites have been fabricated to produce materials that have enhanced strength, increased toughness, improved electrical properties, better thermal properties, and lower densities.

The focus of this work is on the processing and characterization of ceramic composites that lead to superior mechanical properties - structural composites. Whether oxide based or non-oxide based materials, all ceramics are characterized by poor fracture properties. It was with a view to improve the fracture properties of ceramics that considerable effort has been directed towards the development of ceramic composites. Composite materials can be classified as metal matrix composites (MMC), polymer matrix composites (PMC), and ceramic matrix composites (CMC). As can be expected, each of these are operative in certain temperature ranges; ceramics being

the highest, followed by metals and polymers in that order. Some examples of these systems are -

MMC - Al-SiC fiber, Al/Si alloy-SiC.

PMC - Epoxy-Carbon fiber.

CMC - SiO₂-SiC, Al₂O₃-SiC, Si₃N₄-SiC, Al₂O₃-ZrO₂.

Ceramic materials can be processed in a number of different ways.

This study involves fabrication of CMCs using sol-gel processing and the polymer pyrolysis method. A detailed description of these methods is given in the following sections.

1.2 SOL-GEL ROUTES TO CERAMIC MATERIALS

1.2.1 Formation of gels: sol to gel conversion

The production of UO₂ in the mid 1960's from a colloidal dispersion was one of the early examples of ceramic processing using the sol-gel technique. The sol-gel process is one in which a starting sol or a suspension of colloids in a liquid is converted to a gel. It can be effected by (i) polymerization of alkoxides or (ii) dispersion of colloids in a liquid. Sols of gold and UO₂ are examples of the latter process and have been the subject of study for a long time. The sol-gel technique for ceramics processing from alkoxides is a subject of great significance and potential and has been extensively studied in the last few years.

The synthesis and reaction of alkoxides as precursors in the sol-gel process have been reviewed. 1,2 Alkoxides tend to

form oligomers through bridges between similar metals or between different metals (bimetallic, tri, and tetra metallic alkoxides) and are soluble in a large number of compounds and solvents, including water, alcohol, other alkoxides, ketones and aldehydes, halogen and halides, and organic acids. Alkoxides are generally very reactive and are extremely susceptible to hydrolysis. Hydrolysis of some alkoxides leads to the formation of solvated hydroxides or oxides with the formation of alcohol as a byproduct. The first step in the synthesis of ceramic materials is the formation of a polymeric gel from the base alkoxide. This involves (i) a hydrolysis reaction and (ii) a polymerization (condensation) reaction.

Hydrolysis:
$$M(OR)_n + H_2O \longrightarrow M(OH)(OR)_{n-1} + ROH$$

Condensation: 2 M(OH)(OR)_{n-1}
$$\longrightarrow$$
 (RO)_{n-1}MOM(OR)_{n-1} + H₂O
M(OH)(OR)_{n-1} + M(OR)_n \longrightarrow (RO)_{n-1}MOM(OR)_{n-1} + ROH

R represents an alkyl group and M is the element or metal under consideration. These polymerization reactions result in the formation of metaloxane chains or polymer networks and finally yield the corresponding oxide.

Silicon alkoxides have been studied extensively as precursors to silica, both in terms of the mechanism of conversion

of the sol to the gel and the conversion of the gel to the final ceramic. Silicontetraethoxide or tetraethoxysilane (TEOS) is a commonly - used precursor in the synthesis of silica gel.

$$Si(OC_2H_5)_4 + H_2O$$
 \longrightarrow $Si(OC_2H_5)_3OH + C_2H_5OH$
 $2 Si(OC_2H_5)_3OH$ \longrightarrow $(C_2H_5O)_3Si-O-Si(OC_2H_5)_3 + H_2O$
 $Si(OC_2H_5)_3OH + Si(OC_2H_5)_4$ \longrightarrow $(C_2H_5O)_3Si-O-Si(OC_2H_5)_3$
 $+ C_2H_5OH$

These polymerization reactions yield Si - OC_2H_5 siloxane chains or polymer networks and finally the Si - O - Si oxide network. All these reactions take place simultaneously leading to the formation of a gel and can continue for 3-4 weeks after gelation in what is referred to as the aging process.

The parameters that affect the hydrolysis reactions include a) degree of hydrolysis, b) type of alkyl group, c) catalysts, and d) amount of water used.

Yoldas 3,4 has studied the effect of the degree of hydrolysis on the sol-gel reaction products. He defined a degree of hydrolysis, $h = [H_2O] / [M(OR)_n]$, and found that for silicon a linear polymer network is obtained for h<n. If the reactions are carried out under conditions of h>n, gels and 3-D polymer networks are obtained.

Hasegawa and Sakka 5 studied the early stages of the

hydrolysis - polymerization reactions to determine the effect of alkyl groups on the conversion of tetraalkoxysilanes. They suggested that the hydrolysis and polymerization of the alkoxysilanes occur very rapidly and the differences in the alkyl group of the silane have very little effect on the overall reaction.

The rate of the sol-gel reaction steps can be increased considerably by using suitable catalysts. Pope and Mackenzie 6 have studied the role of the catalyst in the sol-gel processing of silica using TEOS hydrolyzed with four equivalents of water in ethanol. The gelation time (arbitrarily chosen as the time to reach a viscosity of 10000 P) was about 1000 hours when no catalyst was used. Upon addition of a catalyst, the gelation time ranged from 12 to 107 hours, depending on the nature of the catalyst. Hydrogen fluoride was observed to have the maximum effect in enhancing the reaction. Hydrogen chloride, HNO₃, H₂SO₄, and NH₄OH were some of the other catalysts used by Pope and Mackenzie. However, the gelation times did not correlate with the pH of the solution, which implies that the actual catalytic mechanism has to be taken into account to explain the reaction kinetics.

Another parameter that influences the sol-gel reaction steps is the amount of water used, represented by many as the molar ratio $R = H_2O$ / Si. Sakka ⁷ observed that low R values (1-2) using TEOS and 0.01 M HCl as catalyst yield a spinnable solution upon gelling, while high R values result in gels that cannot be spun. It is suggested that low R values result in the

formation of linear polymers upon hydrolysis of Si(OC₂H₅)₄, thereby resulting in spinnability, while high R values favor formation of non-linear polymers. Pouxviel ⁸ also studied the solgel reaction of silica by varying R values. With low R values (less than stoichiometric) condensation is slow and all the water is depleted, which in turn leads to the presence of residual Si-OR and Si-OH groups in the network. With medium R values (close to stoichiometric), weakly reactive Si-OR groups exist, and with high R values (excess water), complete hydrolysis takes place resulting in an -OR free species.

1.2.2 Drying of gels: supercritical drying

The aging process results in a sharp increase of viscosity leading to the formation of a gel. At this stage the gel contains large amounts of water and solvent and needs to be dried before futher processing. If this liquid within the gel is removed by simple evaporation, the dried product is called a xerogel. Drying by simple evaporation causes the formation of liquid - vapor interfaces within the gel and can result in collapse of the gel network due to surface tension forces.

Supercritical drying is being increasingly used to produce crack - free dried specimens called aerogels. Surface tension forces are absent at supercritical conditions (no liquid-vapor interface); the fluid within the gel is slowly extracted to yield a crack-free porous body. In 1931, Kistler ⁹ reported the preparation of coherent expanded aerogels of silica, alumina, ferric oxide, nickel oxide, and other organics using ethanol as the

supercritical medium. Subsequently Peri 10 , Teichner 11 , and Zarzycki 12 used methanol as the supercritical fluid to dry silica gels. The critical conditions of methanol are quite severe $(T_c=240^{\circ}\text{C}, P_c=78.5 \text{ atm.})$. To avoid these extreme conditions of temperature, Tewari 13 and Lira 14 have recently used CO_2 as the supercritical medium to remove the solvent from silica gels $(T_c=31^{\circ}\text{C}, P_c=73 \text{ atm.})$.

1.2.3 Densification of gels: gel to ceramic conversion

The dried ceramic material (aerogel) has a low density and must be processed at high temperatures to increase its density. During this heat treatment, the processes that occur include removal of residual -OH and -OR groups by polycondensation and slow disappearance of pores. The collapse of pores and the accompanying densification is most commonly achieved either by sintering or by hot pressing.

In the late 1970's Decottignies ¹⁵ synthesized glass by hot pressing pure silica and silica - boria gels. The gels were dried by controlled heating up to 800°C and the dried product was ground and hot pressed to obtain the dense ceramic. Yamane et al. ¹⁶ successfully prepared fracture-free, dense silica by sintering silica xerogels. Subsequently, Prassas et al. ¹⁷ sintered silica aerogels at temperatures around 1150°C to obtain crack-free monolithic silica.

Bertoluzza et al. 18 characterized the chemical changes

in the gel to glass conversion by Raman and IR spectroscopy. The polycondensation of Si-OH groups in the gel to glass transformation was confirmed by the decreasing intensity of the IR peaks at 960 cm⁻¹ (due to Si-OH stretching) with increasing heat treatment temperature.

The densification of silica aerogels takes place at a temperature greater than 1000°C. The actual temperature of densification depends on the distribution of pores and the hydroxyl content of the gel; a finer pore distribution causes densification at a lower temperature as does a high hydroxyl content. Hydroxyl groups are not completely removed even after heating to 1000°C; this leads to the problem of bloating of the gels. Bloating is caused by hydroxyl groups trapped in the bulk of the matrix under the surface layers which are first densified. In order to prevent bloating, the hydroxyl groups must be removed completely prior to densification. This has been accomplished by treating the gel in a chlorine atmosphere, vacuum ¹⁹, or a fluorine atmosphere ²⁰.

Brinker and Scherer ²¹ suggest that the mechanism of gel densification consists of at least four steps - i) capillary contraction, ii) polycondensation reactions which cross-link the network and expel water, iii) structural relaxation, and iv) viscous sintering. The first three steps cause the skeletal density to increase towards that of silica, and the fourth step eliminates the pores. For silica gels, skeletal densification is proposed to occur between 450 and 600°C with viscous sintering taking

place between 800 and 900°C.

The sol-gel process has been studied extensively in recent years and has been perceived to be a significant route to process ceramic materials. The advantages of the sol-gel process include greater purity, better homogeneity, much lower processing temperatures, ease of forming, and potential for fabricating multiphase matrices. The primary disadvantages are difficulty in drying, high shrinkage, and low yield.

1.3 POLYMER PYROLYSIS ROUTES TO CERAMIC MATERIALS

The concept of synthesizing ceramics from polymers is similar to the synthesis of carbonaceous bodies from organic compounds. The organics are dissolved in a solvent, formed to the desired shape, and converted to a carbon body by heating at a high temperature in an inert atmosphere. Similar heating of an organosilicon polymer can be expected to produce silicon carbide instead of carbon. The polymers that yield ceramic materials consist primarily of C and H atoms along with one or more other atoms such as Si, B, or N. During heating at sufficiently high temperatures, the hydrogen atoms can be stripped off, leaving behind the carbon skeleton and the atoms of the other element (Si, B, N). Some ceramics synthesized by this method include SiC, Si₃N₄, BN, and B₄C. In 1964, Chantrell and Popper ²² discussed the relationship of certain inorganic polymers to ceramics. They indicated the potential of these polymers as structural, refractory,

or electrical materials and suggested the preparation of ceramics in fiber or film form.

In the mid 1970's, Yajima et al. ²³⁻²⁶ directed their efforts towards the synthesis of SiC from the pyrolysis of a polymeric organosilane which they called polycarbosilane (PCS). Polydimethylsilane synthesized from dimethyldichlorosilane was thermally decomposed to form PCS which was melt spun into fibers and cured by oxygen cross-linking. The cross-linked PCS was pyrolyzed at high temperatures to effect the conversion to SiC. The proposed reaction for the conversion of the polymer to the inorganic product is shown below.

$$\begin{pmatrix} CH_3 & H \\ | & | \\ Si & --- & C \\ | & | \\ H & H \end{pmatrix}_n \longrightarrow n SiC + n CH_4 + n H_2$$

Yajima et al. categorized the conversion of PCS to SiC into different temperature ranges. In the first stage (up to 400°C), evaporation of low molecular weight components takes place. In the second stage, dehydrogenation and dehydrocarbonation condensation takes place with an increase in molecular weight. In the third stage, (up to 800°C), decomposition of side chains occurs - dehydrogenation and demethanation, resulting in an inorganic structure with a network of Si-C, C-C, and Si-O bonds. The fourth stage (up to 1200°C) is an extension of the third stage with further development of the inorganic

structure. Crystallization of β -SiC occurs above 1200 °C with growth of crystals as the temperature is increased. The product is nano-crystalline, non-stoichiometric SiC with excess carbon and is now commercially available as Nicalon fibers.

West 27,28 and his colleagues studied the use of a variety of polysilanes including copolymers of dimethylsilane and phenylmethylsilane as precursors for SiC. Their polymers were termed polysilastyrene (PSS) and were of the form $[(Me_2Si)_x]$ PhMeSi]_n where x=0.6 to 1.4. PSS can be photo cross-linked with ultraviolet light and subsequently pyrolyzed to form SiC. The reaction is as follows.

(Ph Si₂ Me₃)
$$\longrightarrow$$
 PhH + CH₄ + 2H₂ + 2SiC

The advantages of synthesizing SiC using this method over that of Yajima's are i) elimination of an intermediate step of producing PCS and ii) elimination of undesirable Si-O bonds by photo crosslinking instead of oxygen cross-linking. Cross-linking of polysilanes by room temperature vulcanization, oxygen curing, photo cross-linking, and thermal/photochemical cross-linking of polyvinyl compounds has been discussed by West et al. ²⁹. Crosslinking of polysilanes by high energy γ -radiation and by use of chemical free radical initiators (CFRI's) has been discussed by Lee and Hench ³⁰.

Other variations of the polymer pyrolysis routes to SiC- based ceramics include incorporation of arylene units in the

main chain of the polysilanes to synthesize a product containing Si-C-H that was thermally stable in oxygen up to 1100°C ³¹. Workers at Union Carbide ³² synthesized branched PCS, vinylic polysilanes, and branched polysilahydrocarbons as precursors to SiC.

Though much of the work in this area in the last two decades has been directed towards synthesis of SiC, precursors for other ceramic systems like Si₃N₄, AlN, BN, and mixed ceramics are being evaluated. Silicon carbide and SiC_xN_y ceramic compositions have been produced at Dow Corning ^{33,34} by use of polysilazane precursors. Seyferth and Wiseman ³⁵ of MIT have worked on Si₃N₄/SiC ceramics from polysilazane precursors. Laine et al. ³⁶ also synthesized Si₃N₄ and Si₂ON₂ from polymer precursors. Paciorek et al. ³⁷ synthesized processable BN preceramic polymers from borazines and subsequently pyrolyzed them in an ammonia atmosphere to prepare BN fibers. Seibold and Russel ³⁸ developed a novel route to AlN ceramics by pressureless sintering of a polyaminoalane precursor.

1.4 CERAMIC COMPOSITES

Important factors that favor development of Ceramic Matrix Composites (CMC) are 1) improved mechanical properties, 2) low density, 3) environmental stability relative to polymers and metals, 4) low cost, and 5) high temperature service. Some problems associated with CMC are 1) high temperature

processing, 2) limited densification, 3) difficulty in fabricating complex geometries (in some cases), and 4) reliability concerns.

Many ceramics have been used in the fabrication of ceramic composites. The most studied materials include SiC, Si₃N₄, and TiC in the non-oxide category; oxide based ceramics studied include SiO₂ (including silicates), Al₂O₃, and ZrO₂. Microhardness, toughness, elastic moduli, and flexure strength are some of the properties used to characterize the mechanical nature of the composite.

1.4.1 Types of Ceramic Matrix Composites

Depending on the nature of the reinforcing second phase, ceramic matrix composites can be further classified as particulate, fiber, and whisker-reinforced composites.

Particulate composites: As the name suggests, particulate composites consist of a matrix phase that may or may not be crystalline and a second phase that is essentially particulate in nature. Some of the factors that affect the properties of particulate composites are compatibility and spatial distribution of particles. Compatibility concerns the thermal expansion mismatch between phases, sinterability of the component phases, and the occurrence of reactions. Spatial distribution of particles can be non-uniform and difficult to control. Some early work on toughening in particulate composites was done by Claussen ³⁹ on the Al₂O₃-ZrO₂ system. Lange ⁴⁰ also observed significant toughening when tetragonal ZrO₂ was present in an Al₂O₃ matrix. The effect of adding TiC particulates on the

toughness and flexure strength of SiC 41 , Al₂O₃ 42 , and Si₃N₄ 43 matrices has been studied. A strengthening of Si₃N₄ was observed by Dutta and Buzek 44 upon addition of YSZ (yttria-stabilized zirconia) particulates.

Fiber and Whisker reinforced composites: Fibers and whiskers constitute another kind of reinforcing materials. Fibers are generally 10-20 μ m or lesser in diameter and have lengths varying up to the order of centimeters. Fibers may or may not be polycrystalline. Whiskers are much shorter, with lengths of about 10 μ m and average diameters of 0.1-1.0 μ m. A whisker is a single crystal and is essentially a much purer form of the same material than a fiber. Examples of some commercially available fibers are listed in Table 1 45 .

Important considerations in the fabrication and use of fiber and whisker reinforced composites are fiber strength, fiber matrix interaction, high temperature oxidation characteristics, and fiber architecture. The fracture strength of the fiber must be higher than that of the matrix. Also, the fiber-matrix bond should neither be too weak nor too strong in order to obtain significant toughening. A serious problem associated with some of the currently available fibers is poor oxidation characteristics at high temperatures. This effectively limits the maximum service temperature of the composite. Lastly, fiber architecture has to do with the orientation of the fiber structure and can be classified as (i) discrete fiber, (ii) unidirectional, 1-D, (iii) planar interlaced, 2-D, and (iv) fully integrated, 3-D.

A number of ceramic systems have been studied using fiber and whisker reinforcements. Buljan ⁴⁶ and Shalek ⁴⁷ have examined the effect of adding SiC whiskers on the toughness and fracture strength of Si₃N₄. SiC whiskers have been incorporated in glass matrices to achieve toughening ⁴⁸. Strengthening and toughening of alumina matrices was observed by Wei and Becher ⁴⁹ upon addition of SiC whiskers. Fibers of SiC have been used to reinforce other ceramic matrices like glass and glass ceramics ⁵⁰, SiC ⁵¹, and Si₃N₄ ⁵².

Table 1. Examples of commercially available ceramic fibers

Designation	Composition
Nicalon	59 Si, 31 C, 10 O
Nextel 312	62 Al ₂ O ₃ , 14 B ₂ O ₃ , 24 SiO ₂
SCS-6	SiC on a carbon core
Tyranno	Si, Ti, C, O
HPZ	59 Si, 10 C, 28 N, 3 O
PRD-166	Al ₂ O ₃ , 15-25 ZrO ₂

1.4.2 Mechanisms of toughening in CMCs

One of the most important mechanical properties is the toughness or the resistance to fracture of the composite.

Toughening is effected by increasing the fracture energy of the material system over that of the monolithic matrix alone. A

number of mechanisms have been proposed to explain the toughening observed in CMCs ⁵³. These include microcracking, crack impediment, crack deflection / fiber pullout, load transfer, and transformation toughening. In CMCs, most of the toughening mechanisms depend on the interaction of an advancing crack with the composite microstructure.

Microcracking: Microcracks can be defined as cracks of the order of microns that most commonly occur due to thermal expansion mismatches. Microcracks can also be generated due to phase transformation and, to a lesser extent, from differences in elastic moduli. They are generated at or near the crack tip, due to the superposition of high tensile stress concentrated near the crack tip and mismatch stresses. This results in a microcracked process zone around the crack tip that leads to an increase in fracture toughness. An increase in fracture energy due to microcracking is directly proportional to the volume fraction of particles that develop microcracks.

Crack impediment: This mechanism of toughening arises from the use of crack - impeding second phase materials. Ductile wires which are not refractory are used to arrest cracks or impede their paths. Best results are obtained with uniaxial fibers arranged parallel with the principal stress.

Crack deflection / fiber pullout: This mechanism is related to crack impediment and microcracking, since these can be important factors in crack deflection. If cracks deflect along the fiber-matrix interface, what is called fiber-pullout often

results. A second form of crack deflection is crack forking into two paths around or through a particle or fiber due to the orientation of fracture surfaces such as grain boundaries or cleavage planes. One requirement for fiber pullout to occur is the existence of the correct bonding strength between the fiber or particles and the matrix. Too strong a bond will not allow pullout to occur and too weak a bond will make the composite susceptible to failure.

Load transfer: Load transfer from a matrix to high strength fibers can occur if the Young's modulus of the fiber is greater than that of the matrix. The extent of toughening increases as the ratio of the moduli increases. Unidirectional fibers give greatest toughening for crack propogation perpendicular to fibers and no toughening for crack propogation parallel to fibers. This toughening mechanism is more significant for most PMCs than for CMCs, since in ceramic systems the moduli are approximately similar.

Transformation toughening: This toughening mechanism arises out of the creation of a "transformed" zone in the matrix and the subsequent interaction of this zone with the matrix. It involves fine particles in an unstable crystal structure that are inhibited from transforming to the stable form. However, in the presence of a crack tip, under high stress, the transformation occurs, resulting in a "transformed" zone along the fracture surface generated by a propogating crack. The strain energy trapped in the "transformed" zone decreases the available energy for crack propogation and thus enhances toughness.

A few examples of probable mechanisms in specific systems are listed below ⁵³. However, it must be noted that more than one mechanism can be operative in any system.

Microcracking - Carbon-Carbon

Crack impediment - Glass-SiC

Fiber pullout - Glass-SiC

Load transfer - Glass-Carbon

Transformation toughening - Al₂O₃-ZrO₂

1.4.3 Processing and Fabrication of Ceramic Matrix Composites

1.4.3.1 Conventional techniques

Extended use of CMCs will ultimately depend on the improvements in processing and fabrication. The important considerations are fabricating at or close to near-net shape, achieving high densities, maintaining fiber integrity, time, and cost.

The fabricating routes to CMCs include powder processing, melt infiltration, chemical vapor deposition, polymer pyrolysis, and to a limited extent sol-gel processing. Irrespective of the fabrication route used, the final step in the process involves a high temperature treatment, which can either be hot pressing or sintering. A brief description of the first three methods is given below.

Powder Processing: This is one of the traditional processing routes to ceramics and ceramic composites. In the fabrication of particulate composites, starting powders of the component phases are mixed together and subsequently either sintered or hot pressed. Zirconia-toughened alumina (ZTA) is a particulate composite fabricated by sintering together micron or submicron-sized particles of zirconia and alumina to result in a structure that is fine-grained polycrystalline alumina with zirconia inclusions. Powder processing has also been employed in the fabrication of fiber composites. A fiber preform is infiltrated with a slurry of the matrix material and the infiltrated body is then dried and hot pressed to yield the final composite. An alternative technique is to mix chopped fibers and whiskers into the slurry, dry the specimen to achieve high densities, and hot press to the final density. This results in a composite with much more uniform properties. This processing route has been employed in a number of systems; the matrices studied include glass ceramics, alumina, and silicon nitride with fibers of carbon and silicon carbide as the reinforcement.

Melt infiltration: This processing route has been primarily used in metallic systems, but its use is now being extended to ceramic systems as well. The advantages include higher densities and little dimensional change of the final product. As the name suggests, melt infiltration involves the infiltration of a fiber preform with a melt of the required matrix. The process can be carried out either under vacuum or under pressure. A key factor is the extent of wetting that occurs between

employed to tailor the wetting behaviour for particular systems. A typical lab scale apparatus is a vacuum hot press that has graphite heating elements to preheat the fiber preform and to melt the matrix material. One significant problem is the onset of thermal expansion mismatch and the volume change upon solidification/cooling which can lead to extensive matrix tensile stresses. A Si-SiC composite and a CaF₂-SiC whisker system has been fabricated by Hillig ⁵⁴ using melt infiltration.

Chemical Vapor Deposition: Vapor deposition refers to the condensation of elements or compounds from the vapor state to form solid deposits. In chemical vapor deposition (CVD), as the name suggests, deposits are formed through chemical reactions in the gas phase. Some of the common ways in which a CVD reaction can proceed are by hydrogen reduction, reduction using metal vapors, pyrolysis and chemical transport. Apart from traditional ceramic materials like SiC, BN, and TiC, fiber reinforced ceramic composites have been fabricated using the CVD technique. Most commonly, the process involves deposition of the matrix phase around a fiber bundle. It is a low temperature that does not damage the fiber, unlike conventional techniques. Chemical vapor deposition-based techniques for ceramic composites can be either isothermal or may utilize a thermal gradient or a pressure gradient or both. Isothermal fabrication may take up to several weeks or months for deposition to be completed. A faster process has been developed at Oak Ridge National Laboratory that yields reasonable densities of about 80% of theoretical in about twenty four hours. ⁵⁵ Important factors to be considered in the CVD process are chemical equilibria, chemical transport, and chemical kinetics.

1.4.3.2 Sol-gel techniques

Lannutti and Clark ^{56, 57} reported the fabrication of CMCs via the sol-gel route in 1984. Short fibers/whiskers of ZrO₂, graphite, and SiC were used to reinforce Al₂O₃ matrices derived from aluminium sec-butoxide. The whiskers dispersed in the sol and "frozen" into the matrix through gelation. The gelled product was dried and fired to form the composite. Additionally, fiber preforms of SiC, Al₂O₃, and ZrO₂ were used to reinforce sol-gel derived matrices of Al₂O₃. While the fibers did not seem to enhance the toughness of the material, the addition of whiskers reduced shrinkage during drying and firing and resulted in moderate toughening. Similar work was done by Lee and Hench ⁵⁸ by using SiC fibers to reinforce gel - derived silica. Chopped fibers of Nicalon (β -SiC) and Silar (α -SiC) were mixed in silica sol containing glycerol or formaldehyde as drying control chemical additives (DCCAs). The mixture was cast, gelled, dried, and fired at 1200°C to form the composite. Like Lannutti and Clark, Lee and Hench had difficulty in densifying the composite.

 SiC/SiO_2 molecular composites were fabricated by mixing polysilastyrene (PSS) with a silica sol followed by cogellation, cross-linking, and pyrolysis at high temperatures 59 .

A maximum SiC loading of 3% by volume of composite was obtained; higher loadings resulted in macroscopic cracking of the specimens. Again, the composite densities were lower than theoretical, but the microhardness of composites heated to 800°C was ~500 DPN compared to ~200 DPN for the monolithic silica matrix. Oi and Pantano 60 fabricated C - fiber reinforced borosilicate glass by hot pressing the sol-gel derived matrix. A was observed for a 15-35% fiber volume porosity of 5-10% fraction composite, and for a fiber volume fraction greater than 35%, densities of less than 90% theoretical were obtained. In spite of the porosity, a maximum fracture toughness of 10 MPa $m^{1/2}$ and a maximum flexural strength (3-point bending) of ~330 MPa was obtained. Recently, Park and Lee 61 included reactive ceramic species like furfuryl alcohol (FuOH), alumina, and chromia in a silica sol to enhance sinterability of the composite.

Proposed fabrication technique: The objective of this study is the production and characterization of SiO₂-SiC composites. The matrix of the composite is aerogel-derived silica and the reinforcing phase is organosilicon polymer derived silicon carbide. The aged silica gels are supercritically dried using CO₂ to form aerogels of low density. Polycarbosilane (PCS), a polymer precursor to SiC is dissolved in a solvent and used to infiltrate the jungle-gym network of pores of the aerogel. After evaporation of the solvent, the infiltrated gel is processed at high temperatures to simultaneously convert PCS to SiC and the matrix to dense SiO₂.

Some of the problems involved in the fabrication of CMCs are (i) difficulty in achieving high densities, (ii) nonuniformity of distribution of the reinforcing phase, (iii) mechanical damage of fibers during hot pressing, (iv) oxidation/ chemical attack of fibers and whiskers during high temperature processing, and (v) extent of bonding at the interface of the matrix and reinforcing phase. This fabrication technique can be expected to alleviate or elimninate some of the problems mentioned above. Achieving high densities of the composite is a problem that pervades every technique used for processing CMCs. It is very difficult to achieve reasonable densities without hot pressing, especially when fibers are used as reinforcements. Secondly, non-uniformity of the composite is a concern when using fibers and whiskers as reinforcements. Whiskers tend to 3-D fiber architecture (for maximum agglomerate and a uniformity) makes densification even more difficult. In this technique, since the SiC phase is generated from a starting liquid of the PCS solution, complete uniformity can be expected. Thirdly, there is no mechanical damage to the reinforcing phase since hot pressing is not used to densify the composite. Since the sol-gel technique is lower temperature process a than conventional techniques, chemical alteration ofthe reinforcements will not be a problem. Lastly, even though there is no direct control of the bonding at the interface, the excess carbon in the residue of PCS pyrolysis can be expected to assist in providing an optimum bonding at the interface.

Chapter 2

MATERIALS AND METHODS

2.1 STARTING MATERIALS

2.1.1 Silica aerogels: preparation and characterization

Silica aerogels used as the matrix in the composite fabrication were processed and studied by Lira and Rangarajan ¹⁴ of the Department of Chemical Engineering, Michigan State University. Silica sol was prepared by mixing 1 mole of TEOS with 10 moles of water and 3.2 moles of ethanol, using 0.9 moles of 70% HNO₃ as catalyst. The sol was cast in molds and allowed to gel for about three to four weeks at room temperature. The wet gel was transferred from the mold to a pressure vessel and was dried by using supercritical CO₂ to remove ethanol.

Crack-free monolithic aerogels of different sizes and shapes were produced. Silica aerogels produced by the above method are highly porous with a density of about 0.20 g/cc. The geometry and dimensions of typical samples are a)cuboids - 2.2 cm. length, 0.8 cm. height, and 0.8 cm. width, b)cylinders - 2.5 cm. length and 1 cm. diameter, c)small bars - 6 cm. length, 1.5 cm. width, and 0.15 cm thickness, and d)big bars - 8.5 cm. length, 1.6 cm. width, and 0.3 cm. thickness. Aerogels were then stored in a dessicator before further use to prevent contact with ambient moisture.

Mercury porosimetry was used in an attempt to estimate the mean pore size, pore size distribution, and density of silica aerogels. The basis of mercury porosimetry is the penetration of liquid into a capillary as applied to a non-wetting liquid like mercury. The size of a pore is directly proportional to the pressure needed to force mercury into it; the relationship governing this behaviour is a modification of the Young and Laplace equation.

$P = 2 \gamma \cos \theta / r$

Here P=applied pressure, r=radius of the pore, γ =surface tension of mercury, and θ =contact angle. For a given pressure, the diameter of the pore is known, and based on the intrusion data, the volume of the pore can be determined. A Micromeritics poresizer (Model 9310) having a maximum pressure capability of 30,000 psi was used.

Nitrogen adsorption was used to measure the mean pore surface area of silica aerogels. The BET equation is used to relate the pore surface area to the volume of nitrogen adsorbed. It is given as follows.

$$S = V_m AN/M$$

where S=pore surface area, V_m =volume of gas(STP) required to form an adsorbed monolayer, A=Avogadro number, N=area of each adsorbed gas molecule, M=molar volume of gas. If V=volume of gas (STP) adsorbed at pressure P, and P_0 =saturation pressure or the vapor pressure of the liquified gas at the adsorbing temperature, V_m is found from the slope and intercept of a plot of $P/V(P_0-P)$ vs P/P_0 .

A preliminary evaluation of the behaviour of the aerogel upon heat treatment was studied by thermogravimetric analysis (TGA) and by Fourier Transform Infrared Spectroscopy (FTIR). A TGA is most commonly a plot of weight loss versus treatment temperature. Based on the profile, information on chemical changes/reactions (loss of water, combustion of organics, etc.) over specific temperature ranges can be obtained. The FTIR spectrum is typically a plot of absorbance% versus wavenumber of the radiation. The KBr pellet technique was used to prepare specimens for analysis. About 1 mg of the specimen was finely ground and mixed with about 100 mg of KBr. The mixture was then pressed in a special hand press to form a

transparent thin disk, which was mounted in the spectroscope for analysis. Prior to running the spectrum of the specimen, a blank run using a disk of KBr was done.

A Sartorius microbalance and a DuPont Thermal Analyzer were used to obtain TGA information, while FTIR information was obtained using a Perkin Elmer 1800 spectroscope.

2.1.2 Polycarbosilane: characterization

Polycarbosilane polymer (PCS) is manufactured in Japan by Nippon Carbon Co., Ltd., and is distributed in North America by Dow Corning Corp., Midland, Michigan. PCS is a pale yellow solid at room temperature and is soluble in hexane and tetrahydrofuran.

Initial experiments were conducted to determine the maximum solubility of polycarbosilane in hexane.

The decomposition of polycarbosilane upon heat treatment, resulting in the formation of the inorganic residue, was studied by TGA and FTIR.

2.2 PROCESSING METHOD

2.2.1 Pre-densification of silica aerogels

The highly porous silica aerogels are mechanically weak and in order to make them suitable for subsequent processing, their mechanical integrity needed to be improved. This was accomplished by a pre-densification step, the first step in the processing of the composite.

Pre-densification involves controlled heating of the aerogel to a temperature ranging from 1000 °C to 1100 °C (close to where sintering takes place) and holding at this temperature for 12 hours, resulting in an increase in the gel density. The actual temperature of pre-densification was chosen such that the density of the pre-densified gel was about 1.00 g/cc. This represented a gel that could withstand infiltration of PCS.

Silica aerogels of all geometries except big bars were pre-densified by heating at 5°C/min.; the big bars were pre-densified by heating at 1.6°C/min. All aerogels were pre-densified in a nitrogen atmosphere. The MRL Thermtec furnace described in section 2.3 was used. Upon completion of pre-densification, the furnace was cooled at the rate at which it was heated up. The total run time, for pre-densification at 1.6°C/min. up to 1050°C and holding for 12 hours, is about 32 hours. The temperature controller settings that were used are as follows:

LEFT	CENTER	RIGHT
Pb-8%	Pb-34%	Pb-0.50%
t _i -200s	t _i -1700s	t _i -60s
t _d -15s	t _d -180s	t _d -10s
H _L -25% start then 85%	H _L -100%	H _L -25% start then 85%

2.2.2 Polycarbosilane infiltration

The second step in the processing of the composite is the infiltration of the polymer precursor to SiC, polycarbosilane, into the matrix of the aerogel. Fricke and Reichenauer ⁶² proposed an aerogel structure (Figure 1) with large primary particles and porous secondary particles which form a branching and interconnecting network. With such an open structure, easy infiltration of the polymer into the matrix can be expected.

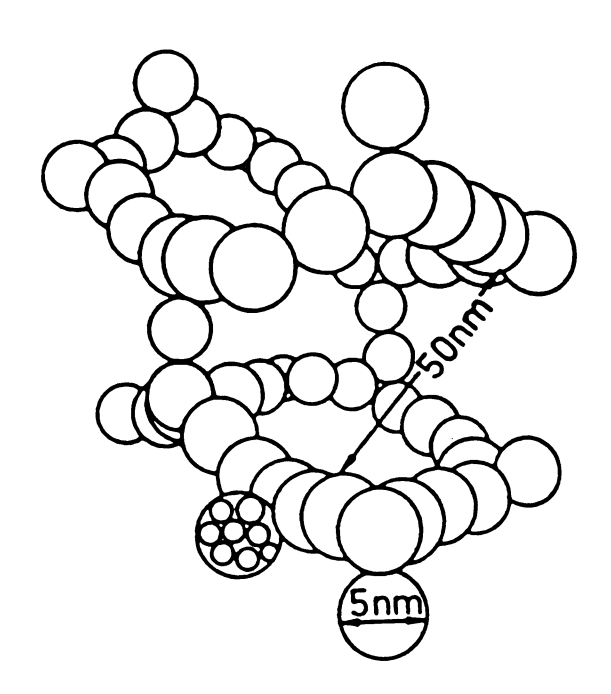


Figure 1. Structure of silica aerogel (from Ref. 62)

Polycarbosilane was dissolved in hexane to form a solution of known concentration by weight. All concentrations are on a weight basis referred to the solution. Concentrations of PCS up to 60 weight% were used in the infiltration process. It was observed that the PCS solutions of concentrations less than 50 weight% could be infiltrated into the porous matrix of the predensified aerogel by simple immersion in atmospheric conditions. Higher temperature infiltrations (70°C) were used with PCS

weight. With such concentrations, the PCS solution became very viscous and higher temperatures reduced the viscosity. After the infiltration was visibly complete (a few minutes), the aerogel was allowed to soak in solution for five additional minutes. The infiltrated aerogel was then removed from the solution with tweezers and set on a sheet of weighing paper. The gel was lightly rinsed with hexane to remove excess polymer from the surfaces. The infiltrated gel was left in air overnight to remove hexane. The infiltration procedure for processing big bars is explained below.

Infiltration conditions for processing big composite bars containing 7% PCS were slightly different. Since the top surface of these bars was not flat, it was not possible to accurately determine the density after pre-densification. A multiple-infiltration step was used to obtain gels containing 7%PCS by weight. Silica aerogels were stored for one week after drying and were pre-densified at 1050°C with a 12-hour hold time. The pre-densified gels were infiltrated first with a 50 weight% PCS solution in hexane. The infiltrated specimen was dried in an oven at 70°C to remove hexane. After no weight change was recorded (hexane removed), the specimen was cooled in the ambient for 10 minutes and infiltrated again with a 50% PCS solution. The above process was repeated and the gel was infiltrated for the third time with a 45% PCS solution. The infiltrated gel was removed from the solution and was left overnight in air.

2.2.3 Cross-linking of polycarbosilane

The polycarbosilane infiltrated into the aerogel matrix was cross-linked before it was pyrolyzed to form SiC. As discussed in the earlier section on polymer pyrolysis routes to ceramic materials, a number of cross-linking techniques have been employed. Oxygen/air cross-linking of PCS is one of the simplest methods and was employed by Yajima et al.²⁵ to cross-link fibers of polycarbosilane. Slow heating of the specimen in air, to a temperature between 200 and 250°C, caused the PCS to cross-link.

The infiltrated silica gel matrices were cross-linked by heating at 0.5°C/min. in 1 atm. air to a temperature between 200 and 250°C and holding at this temperature for 30 min. The total run time for cross-linking at 240°C and holding for 30 min. is about 8 hours.

The MRL Thermtec furnace was used to cross-link the specimens. The temperature controller settings that were used are as follows:

LEFT	CENTER	RIGHT
Pb-8%	Pb-50%	Pb-0.50%
t_i -200s	t _i -1700s	t _i -60s
t _d -15s	t _d -180s	t _d -10s
H _L -10%	H _L -100%	H _L -10% start
		then 15%

2.2.4 Pyrolysis of polycarbosilane and densification of the silica aerogel matrix

Pyrolysis is a high temperature process that results in the conversion of the polymer to a corresponding inorganic material. The different stages in pyrolysis of PCS have been discussed earlier. The infiltrated silica aerogel containing crosslinked polycarbosilane interspersed in its matrix was heated to simultaneously pyrolyse PCS to SiC and densify the silica matrix. An MRL Thermtec furnace described in the next section was used for this last step in the composite fabrication method. All infiltrated green composite specimens were heated at 1.6°C/min. in a nitrogen atmosphere up to a maximum temperature of 1350°C and held at the maximum temperature for 1 hour. Silica aerogels without any polycarbosilane were heated at 5°C/min.(1.6°C/min. for big bars) up to 1250°C and were held at 1250°C for 10 minutes to yield dense silica. The furnace was cooled down to ambient at the rate at which it was heated up and the specimens were removed. The temperature controller settings for the pyrolysis process were the same as those used for the predensification of aerogels.

2.3 HIGH TEMPERATURE MUFFLE TUBE FURNACE

An MRL Thermtec three-zone horizontal muffle tube furnace with a maximum working temperature of 1500°C was used for the composite fabrication steps (pre-densification, cross-linking, and pyrolysis/densification). A Eurotherm Type 812

temperature controller is used on the middle zone and the end zones are controlled by Eurotherm Type 810 controllers.

An inner alumina work tube with one end closed was inserted into the main tube of the furnace. The specimen was placed inside this inner tube on top of a tube dee, which provides a flat surface. The work tube assembly is shown in Figure 2. The inner work tube, the thermocouple (TC) protection tube, and the tube dee are all made of alumina (grade 998-99.8% alumina). All were obtained from McDanel Refractory Company, with the exception of the tube dee which was purchased from Coors Ceramic Company. A stainless steel seal with a Viton gasket, to close the end of the work tube and to provide for the inert gas flow, was obtained from McDanel Refractory Company. A stainless steel fitting was made to house the TC tube, the details of which are shown in Figure 3. Disks of about 2 inch diameter and 1 inch thickness, made from K-30 alumina firebrick, were used as radiation shields. A 1/8" Inconel tube was used as the nitrogen gas inlet to the furnace.

Figure 3 shows details of the seal assembly. The TC tube was joined to the SS fitting by a Dow Corning sealant, SILASTIC 732. The overall schematic of the furnace and the associated experimental apparatus is shown in Figure 4.

The temperature inside the furnace was closest to the set point (about 10°C higher) over a length of 4", starting from a point 20" from the end of the work tube. The specimen was placed on the tube dee on top of a thin bed of alumina powder. The

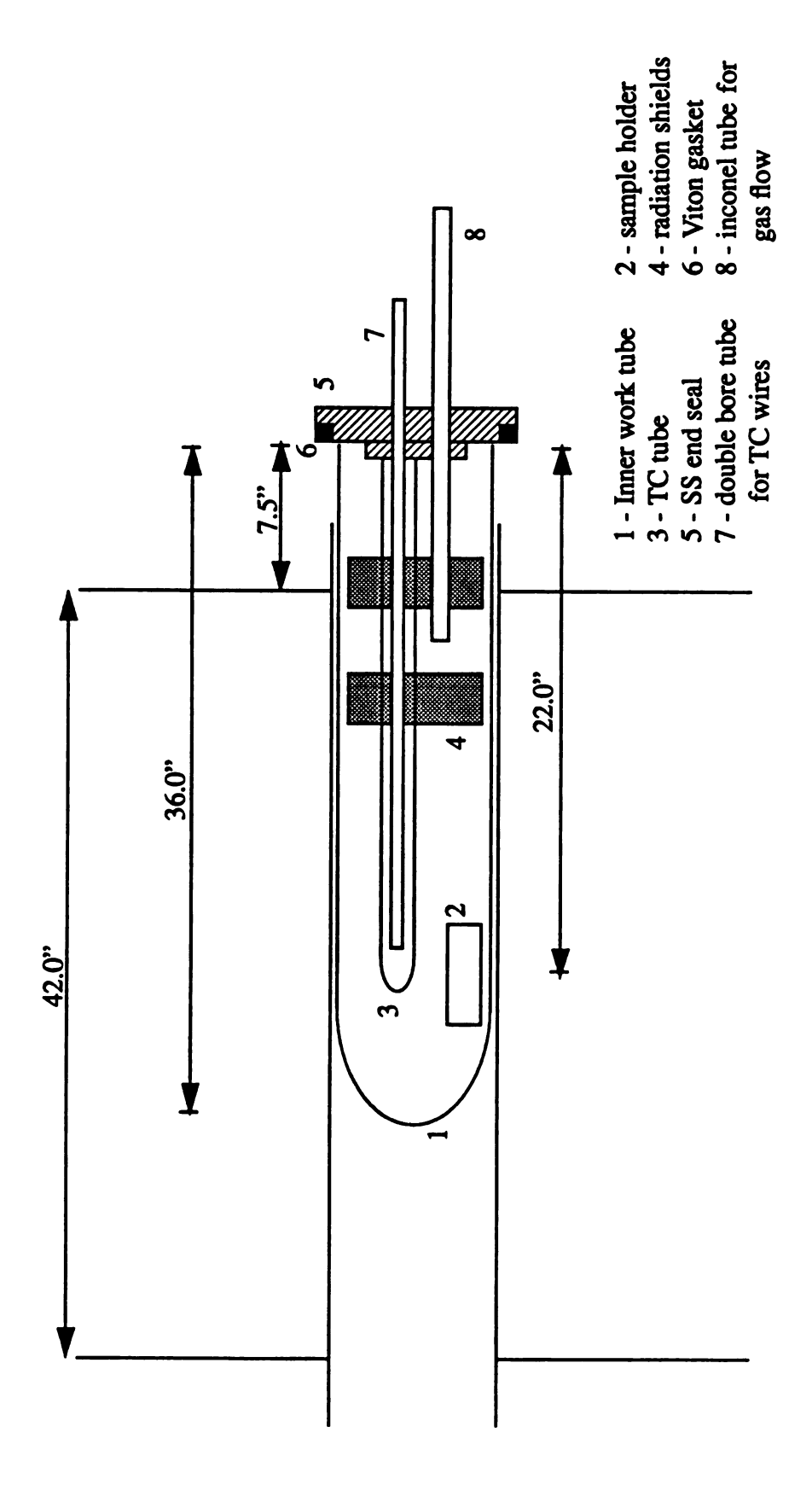


Figure 2. Work tube assembly

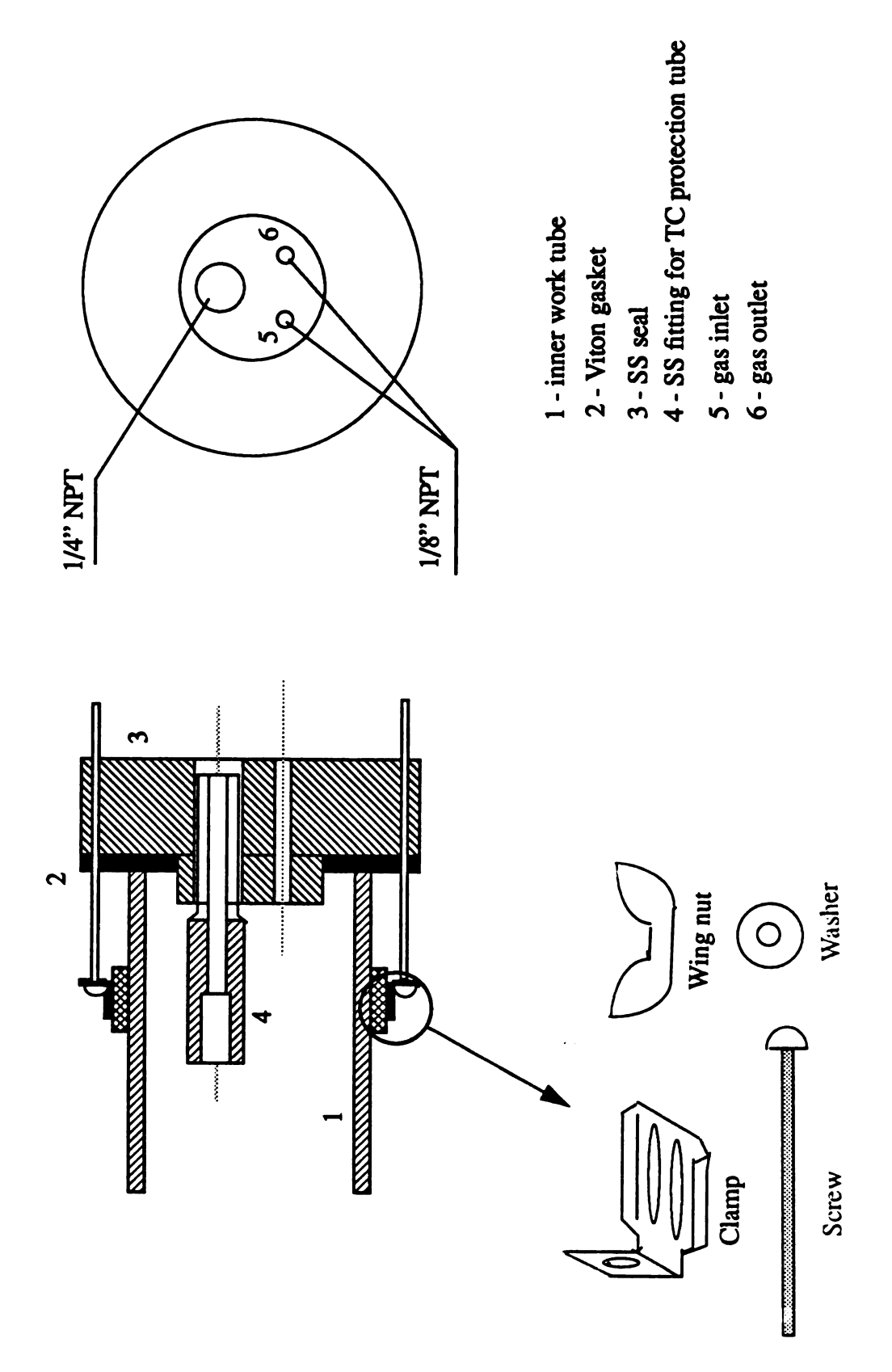


Figure 3. Seal assembly

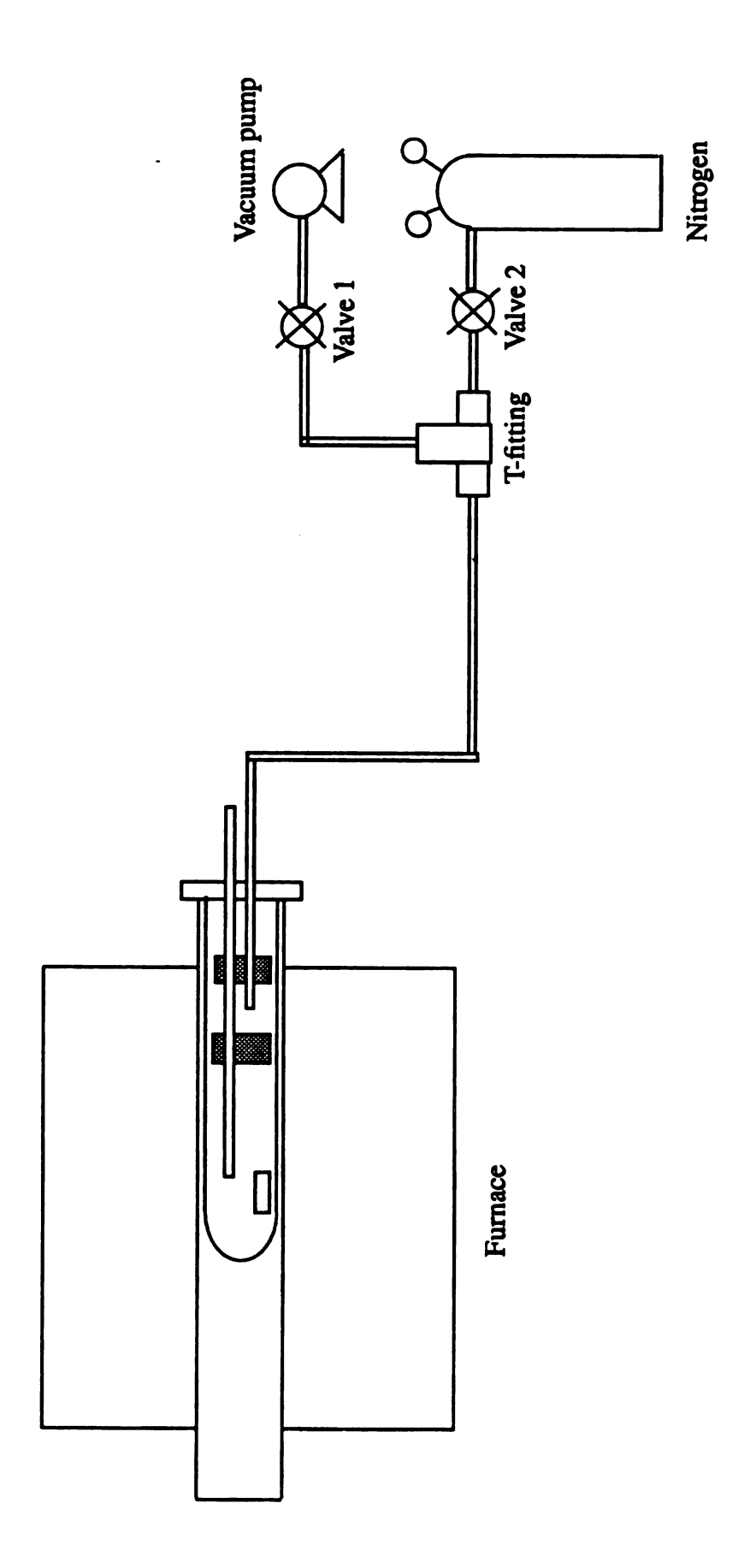


Figure 4. Inert gas flow arrangement

specimens were then covered with a layer of alumina powder. When cuboidal and cylindrical specimens were processed, a rectangular alumina boat (grade 998) was inverted and was used to cover the specimens on the dee. In the case of bars, the rectangular boat was used as a weight on the bars, to prevent warping and bending of the bars. The dee with the specimens was loaded in the furnace such that the center of the specimens was 22" from the end of the work tube. Typically, 4-6 cuboidal specimens or 4 cylindrical specimens, or 2 big bars can be processed at a time. The end of the work tube was sealed and the gas connections were made (Figure 4). Valve 1 was opened and the furnace chamber was evacuated. The vacuum pump was allowed to run for 15 minutes. Valve 1 was closed and chamber was flushed with nitrogen for a few minutes by opening Valve 2. Valve 2 was closed and the above procedure was repeated. After evacuation for the second time, a constant flow of nitrogen of 2.4 liters/min. was maintained and the heat-up cycle was started.

The above procedure was employed for the predensification step. In the case of cross-linking and subsequent pyrolysis/densification, the above procedure was followed up to the sealing of the work tube. The gas connections were not made since cross-linking of PCS needed to be done in air. The furnace was heated up with controller settings given in section 2.2.3 (cross-linking of polycarbosilane). After completion of cross-linking, the gas connections were made, the above process of evacuation/nitrogen purge was done, and the heat-up cycle for pyrolysis was started.

2.4 CHARACTERIZATION OF THE COMPOSITE

Composites of SiO₂/SiC were fabricated by the above method with different PCS loadings in the infiltration step. The effect of varying PCS concentrations on some properties of the composite was studied.

Bulk density is one characteristic that determines whether or not the ceramic composite will be structurally superior to the monolithic matrix. In the fabrication of CMCs, achieving high densities is a significant problem unless hot pressing methods are employed.

FTIR was used to obtain a qualitative analysis of the composition of the SiO₂/SiC composite.

Microstructural characteristics and some mechanical properties of the material system (elastic modulus, microhardness) are being studied by Mr. C.-C. Chiu of the Metallurgy, Mechanics and Materials Science Department, Michigan State University 63.

Chapter 3

RESULTS AND DISCUSSION

3.1. RESULTS OF INITIAL EXPERIMENTS ON SILICA AEROGELS AND POLYCARBOSILANE

The results of initial experiments on silica aerogels and polycarbosilane are discussed separately in the following sections.

3.1.1 Initial experiments on silica aerogels 3.1.1.1 Mercury porosimetry of silica aerogels

Silica aerogels produced in this study are highly porous, with a bulk density of 0.20 +/- 0.02 g/cm³. The size distribution of macropores in these aerogels was determined using mercury porosimetry, the results of which are shown in Table A1.

The mean pore size is 0.05 microns and the macropore surface area is 225 m²/g. The results obtained by mercury porosimetry are not very meaningful because compression of the delicate gel structure resulted, upon intrusion of mercury, and the pore size distribution is therefore not the true one. The reliability of aerogel pore size information as obtained by mercury porosimetry has been discussed by Fricke et al ⁶². It is, however, being used by many to derive a general idea of the aerogel structure.

3.1.1.2. Nitrogen adsorption on silica aerogels

The BET specific surface area of aerogels was determined by nitrogen adsorption. Specific surface area was calculated to be about 425 m²/g. Results of nitrogen adsorption are shown in Figure 5.

3.1.1.3. Behaviour of silica aerogels upon thermal treatment - TGA and FTIR studies

The conversion of silica aerogel to dense silica was studied using TGA and FTIR. A typical TGA profile of silica aerogel heated at 10°C/min. in a nitrogen flow of 50 cc/min. is shown in Figure 6. Up to 150°C, there is an 8% weight loss followed by an additional 5% loss up to 450°C. Upon heating to 600°C, there is a 17% weight loss and at 1000°C, the total weight loss is 21%.

To account for the loss in weight, FTIR studies were conducted on silica aerogels heated at elevated temperatures. Figure 7 shows the FTIR scan of silica aerogel. The broad band in

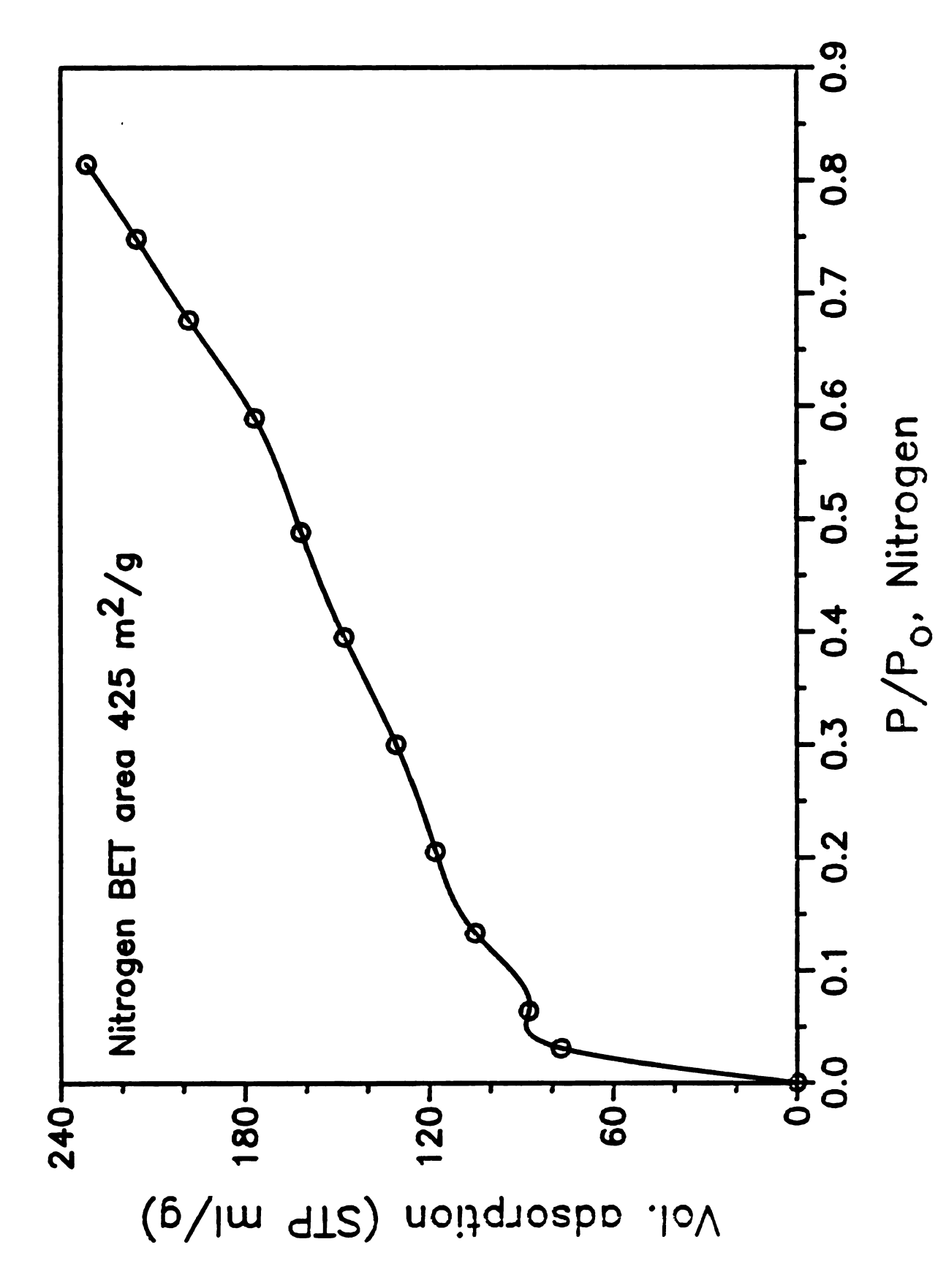
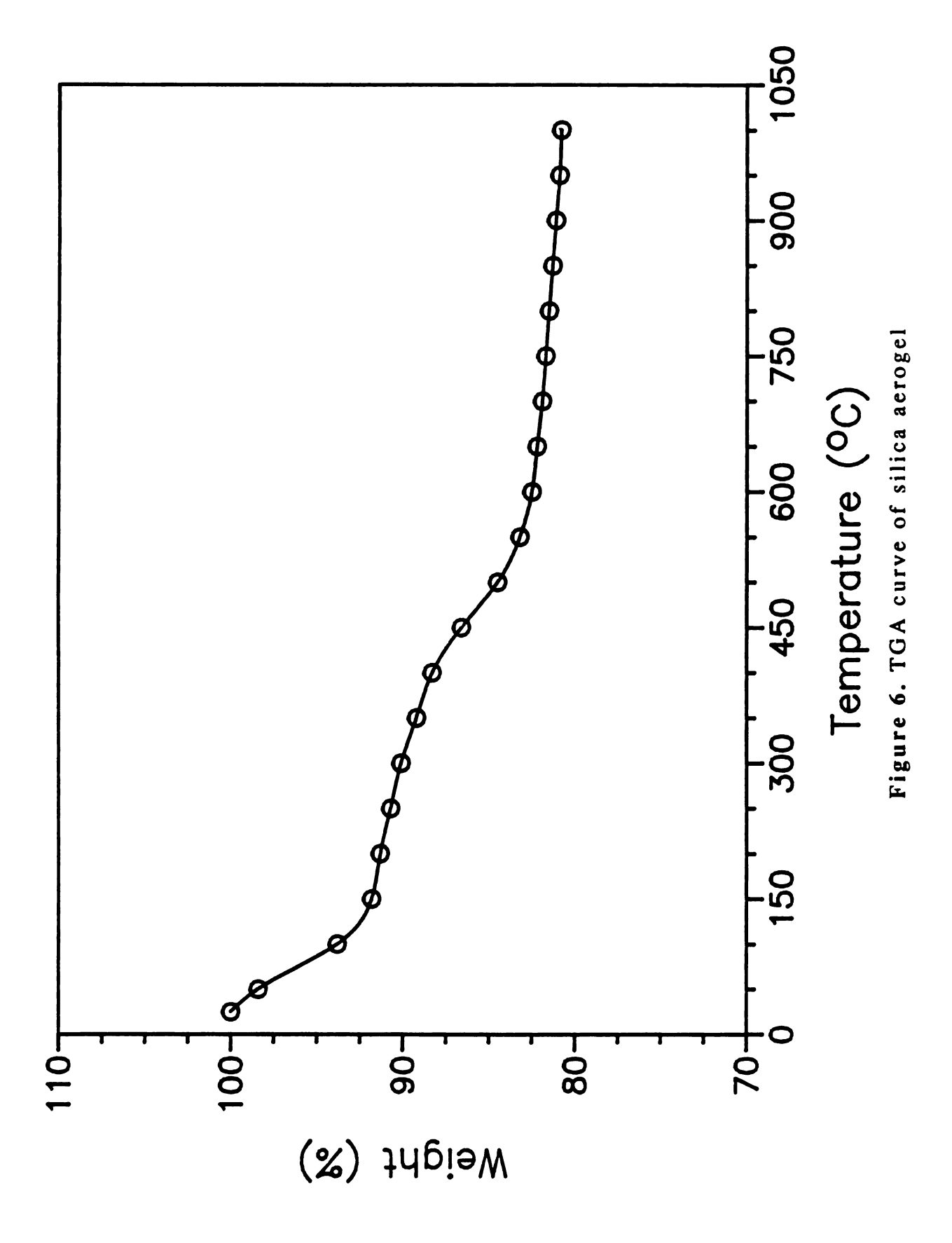


Figure 5. BET adsorption isotherm of silica acrogel



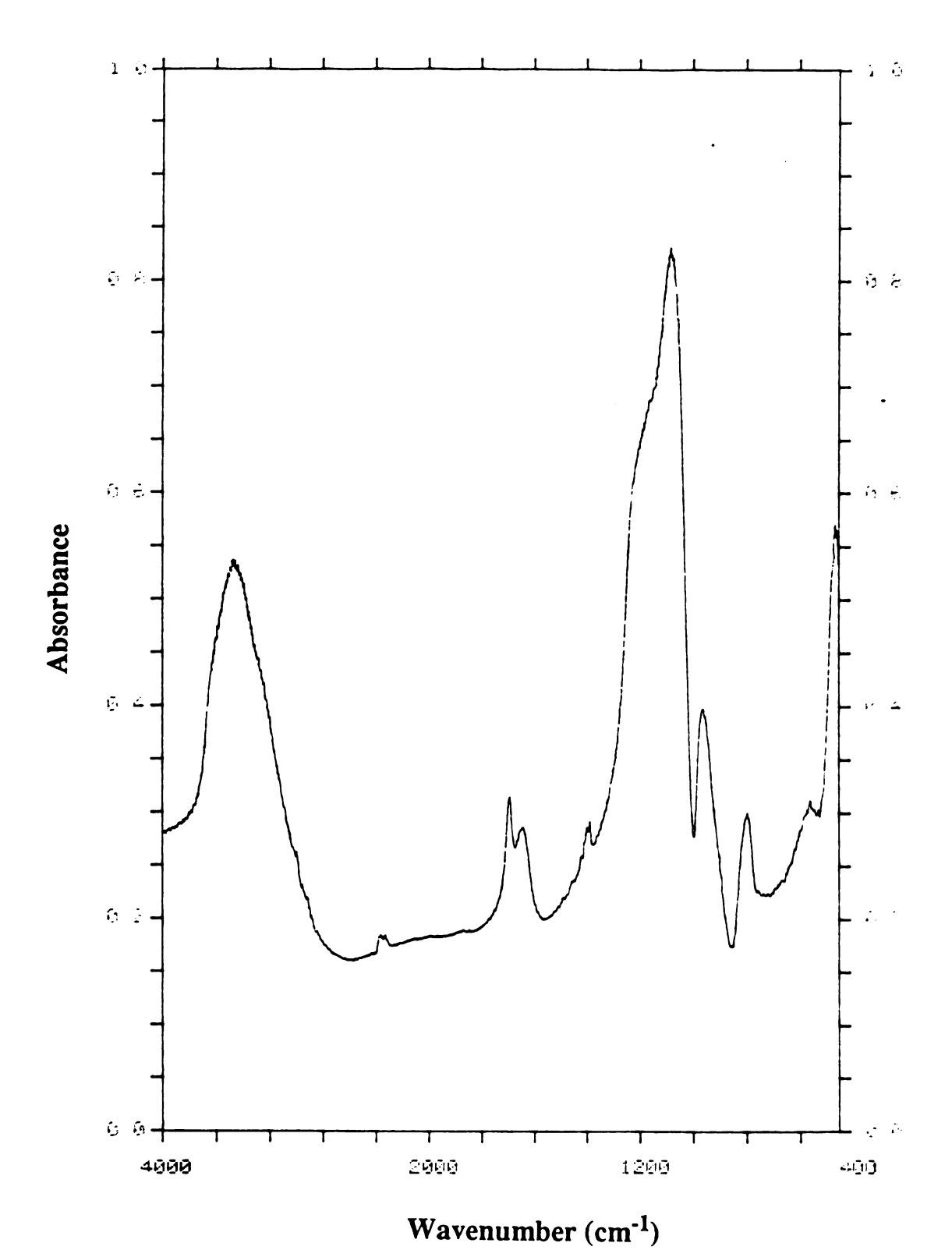


Figure 7. FTIR spectrum of silica aerogel

the 3200-3800 cm⁻¹ region is due to stretching of adsorbed water and the stretching of hydrogen bonds between silanol groups and between Si-OH and water. Bending of molecular water shows up at 1620 cm⁻¹ and an Si-O overtone is seen as the 1640 cm⁻¹ peak. Si-O stretching is manifested as the 1085 cm⁻¹ peak while Si-OH stretching shows up at 960 cm⁻¹. The 800 cm⁻¹ peak is associated with Si-O-Si stretching and the peak at 580 cm⁻¹ corresponds to Si-O bending. Si-O-Si-O deformation shows up as the peak at 465 cm⁻¹.

The FTIR spectrum of dense silica obtained by heating the aerogel to a temperature of 1250°C is shown in Figure 8. The three peaks that remain are those at 465 cm⁻¹ (Si-O-Si-O deformation), at 800 cm⁻¹ (Si-O-Si stretching), and at 1085 cm⁻¹ (Si-O stretching). The FTIR spectra of aerogels heated to intermediate temperatures show a progressive decrease and disappearance of peaks due to Si-OH stretching and Si-O bending. In most of the spectra there is a peak at 2360 cm⁻¹ which is attributed to the molecular vibration of CO₂. This is an artifact that is removed if the specimens are scanned for a longer period of time.

Based on the TGA and FTIR information, the 8% weight loss upon heating to 150°C can be attributed to the removal of water. At 450°C and at 600°C, loss of water continues to take place, accompanied by removal of the -CH₃ groups and the -OH groups. For samples heated to 1050°C, there is a small band due to

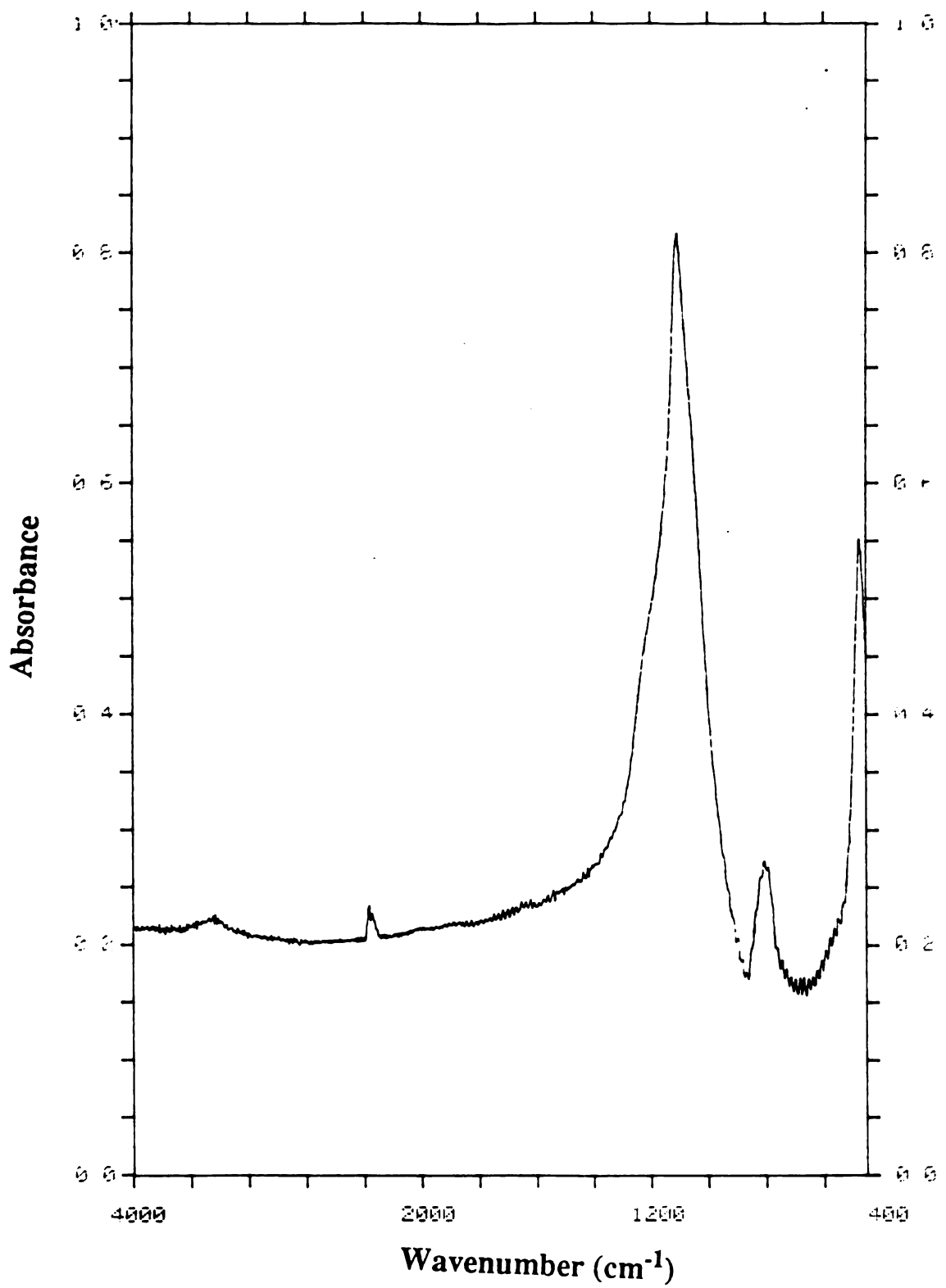


Figure 8. FTIR spectrum of silica aerogel heated to 1250°C (dense silica)

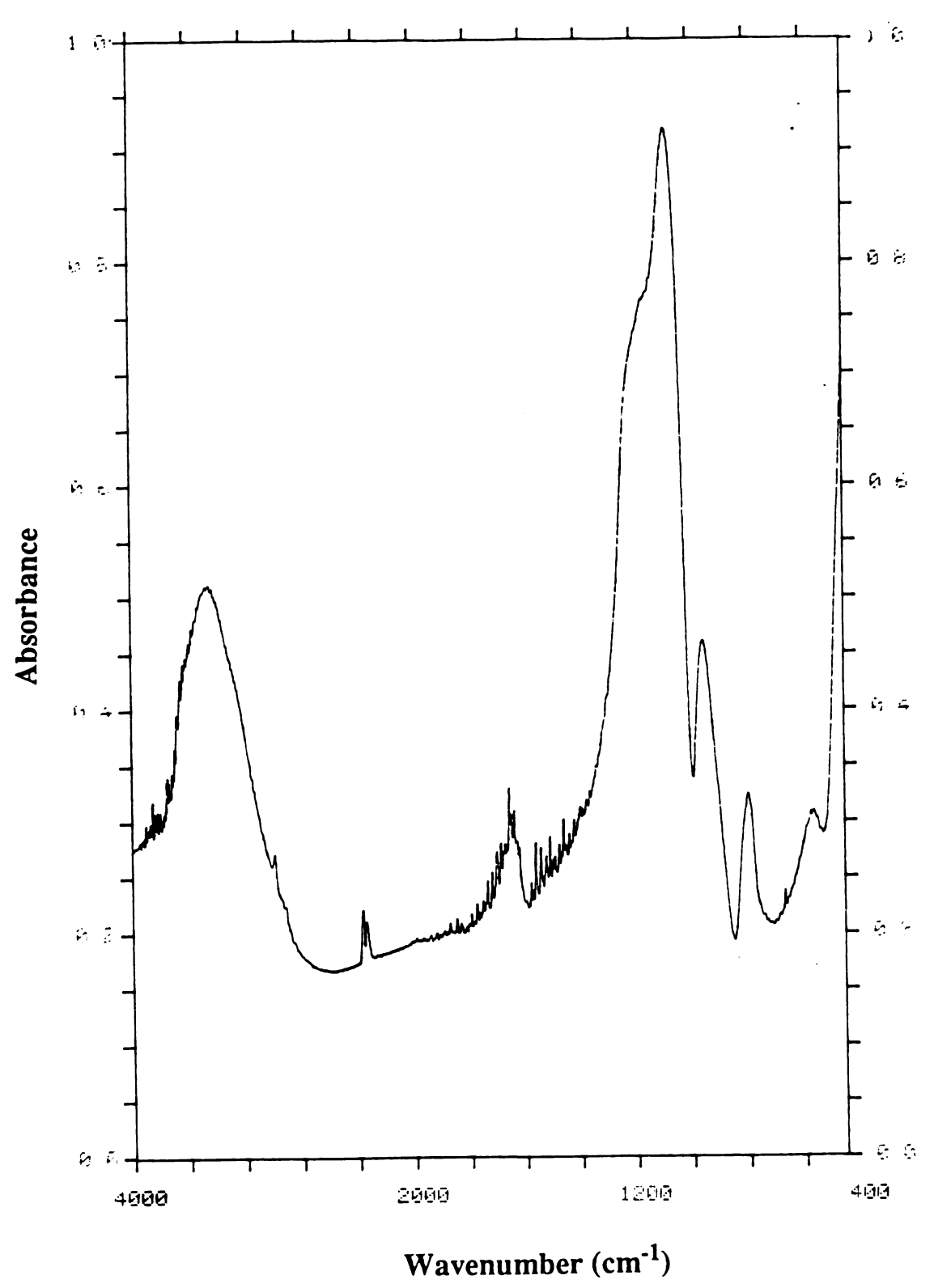


Figure 9. FTIR spectrum of silica aerogel heated to 150°C

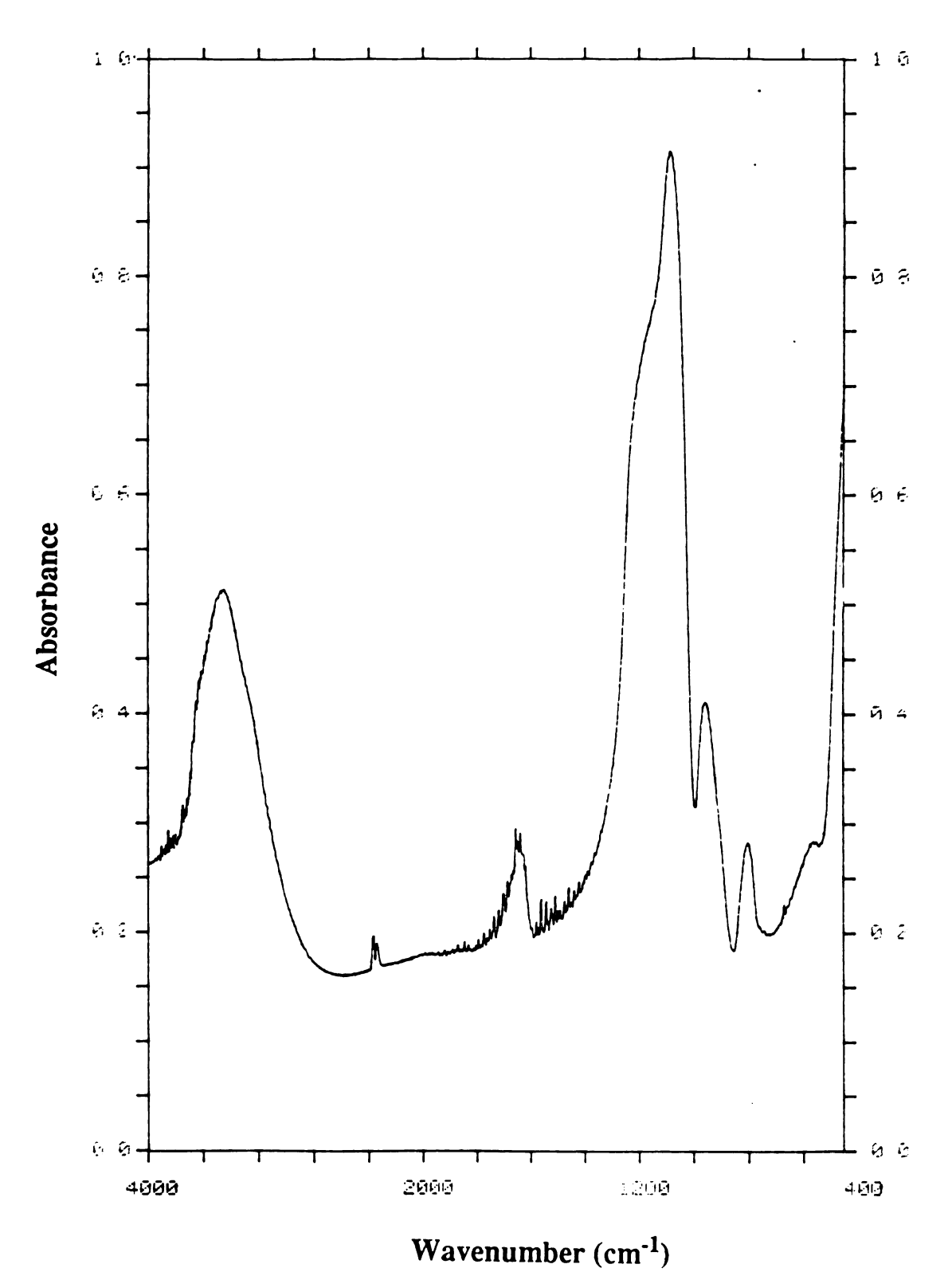


Figure 10. FTIR spectrum of silica aerogel heated to 450°C

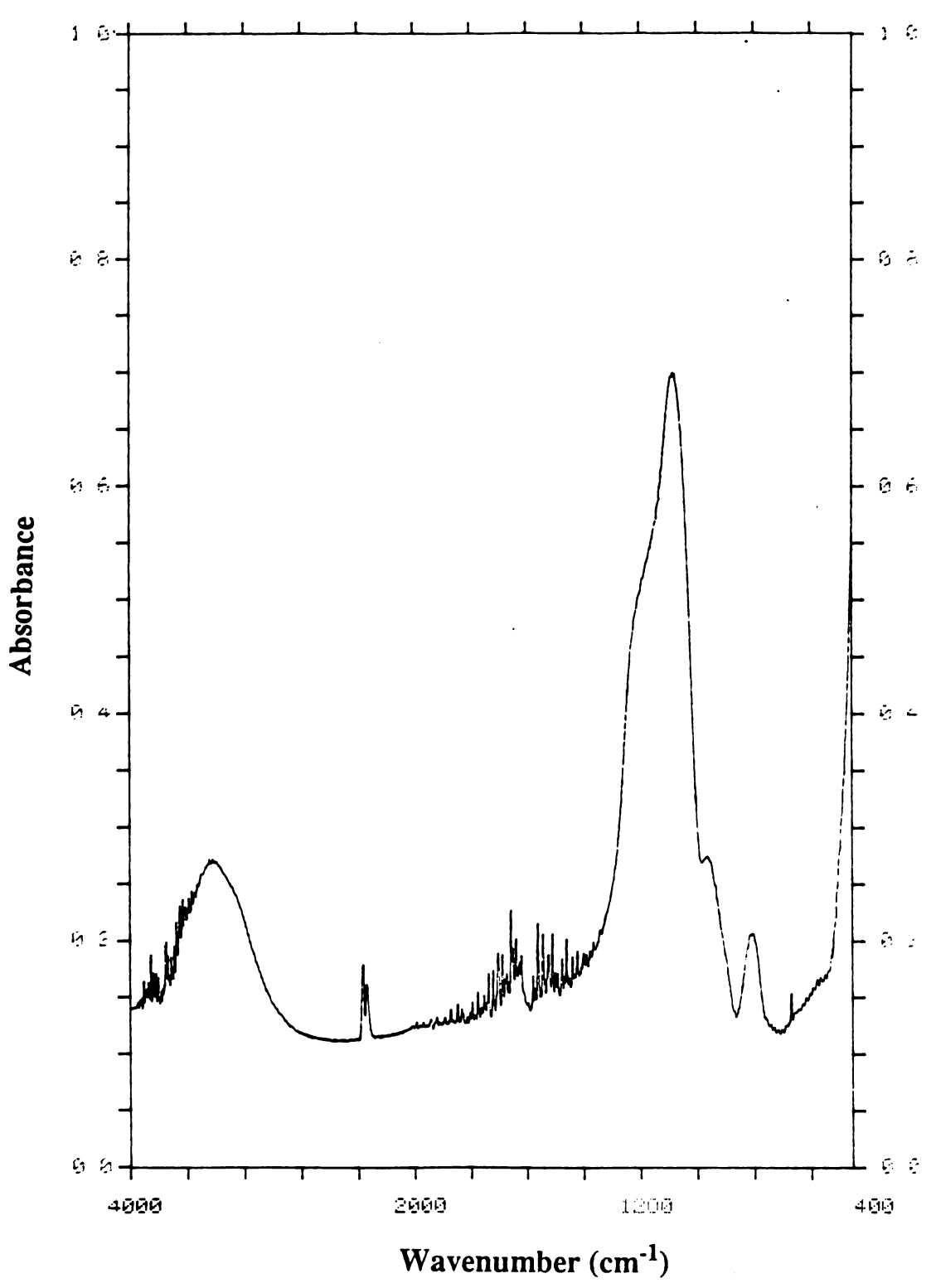


Figure 11. FTIR spectrum of silica aerogel heated to 600°C

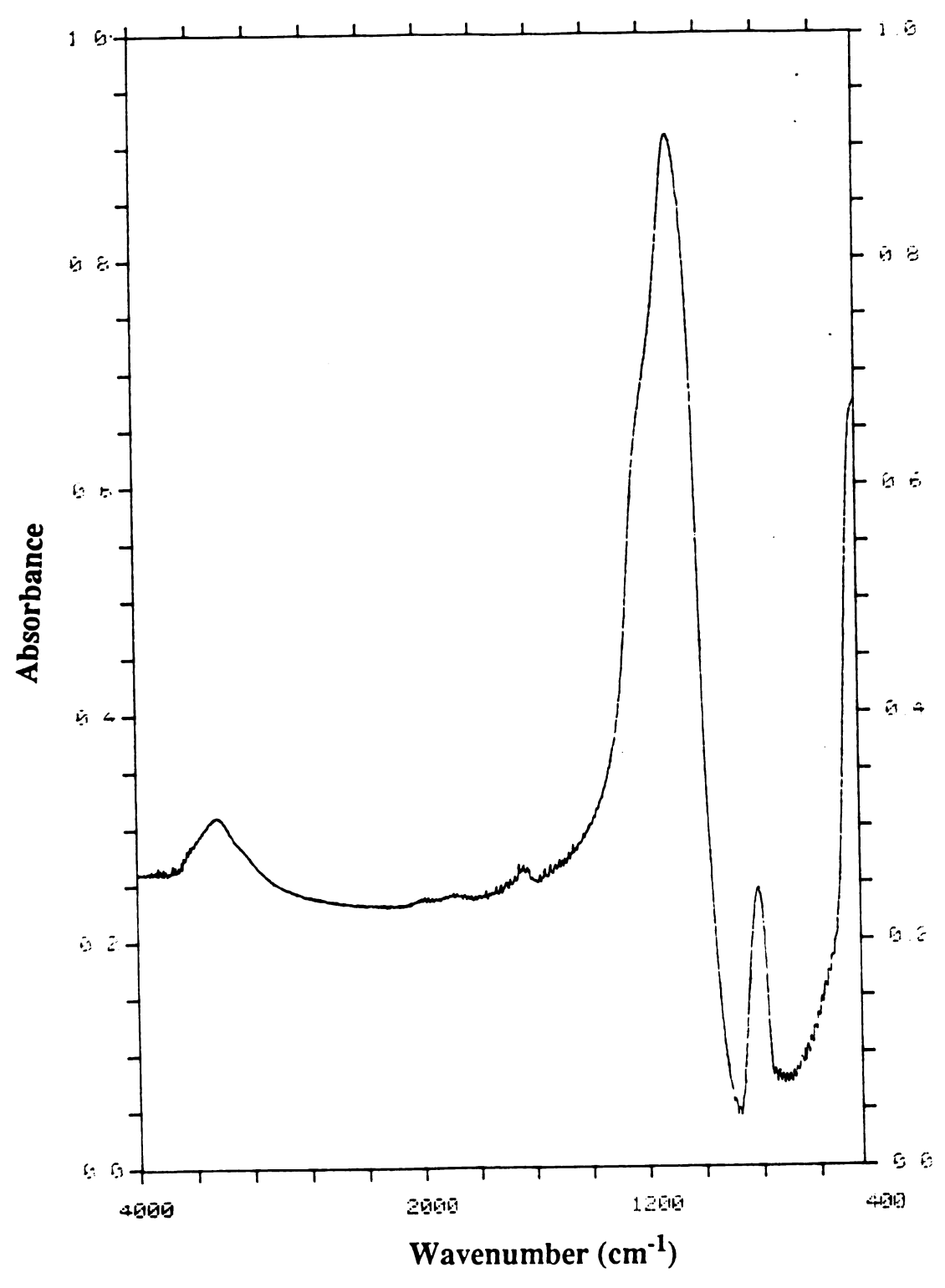


Figure 12. FTIR spectrum of silica aerogel heated to 1050°C

the -OH groups and -CH₃ groups, both of which are further reduced upon heating to 1250°C.

3.1.2 Initial experiments on polycarbosilane 3.1.2.1. Solubility of PCS in hexane

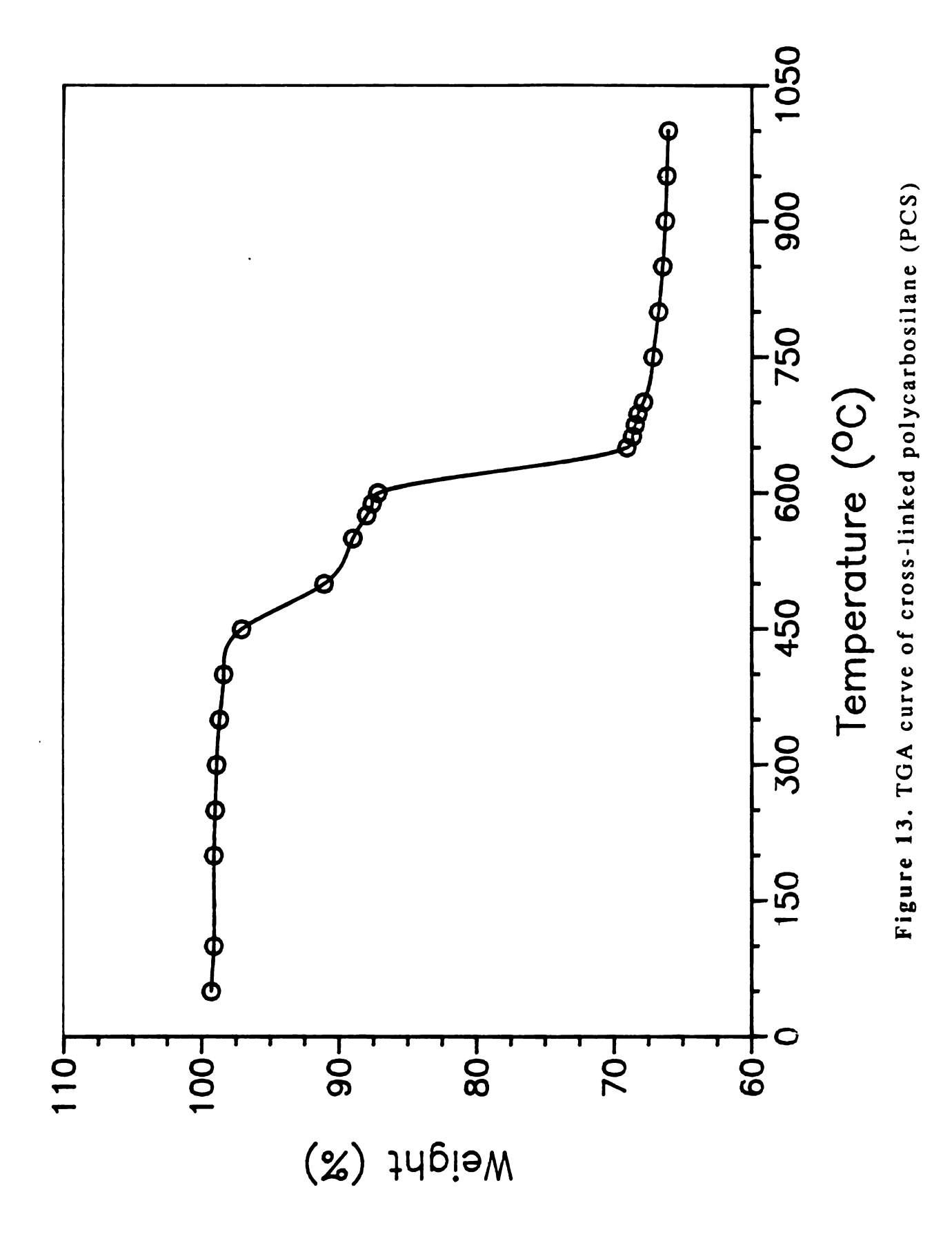
The solubility of polycarbosilane in hexane was determined both at room temperature and at 70°C. Higher temperature infiltration was used to reduce the viscosity of solutions containing greater than 50% PCS by weight. PCS solubility information is listed in Table 2.

Table 2. Polycarbosilane solubility information

Temperature (°C)	Conc. of PCS in hexane (wt%)	Solubility conditions (time, viscosity)
22	< 30	fast, least viscous
22	30-50	slow, moderately viscous
22	50-60	very slow, highly viscous
70	50-60	slow, moderately viscous

3.1.2.2. Behaviour of PCS upon thermal treatment - TGA and FTIR studies

The conversion of PCS to SiC was studied using TGA and FTIR. Figure 13 shows a TGA curve of cross-linked PCS heated at 5°C/min. in a nitrogen flow of 50 cc/min. There was a



9% weight loss upon heating to 500°C. At 650°C, PCS undergoes a 30% weight loss, beyond which the loss in weight is very low (an additional 3%).

An FTIR scan of cross-linked PCS is shown in Figure 14. Peaks at 2950 and 2895 cm⁻¹ peaks are associated with C-H stretching of Si-CH₃. Si-H stretching shows up as a peak at 2100 cm⁻¹. The peaks at 1410 cm⁻¹ and at 1360 cm⁻¹ have to do with CH₂-deformation while the 1250 cm⁻¹ peak is associated with Si-CH₃-deformation. CH₂-wagging in Si-CH₂-Si shows up as a peak at 1020 cm⁻¹. Finally, the peak at 825 cm⁻¹ is attributed to Si-C stretching and Si-CH₃ rocking.

PCS heated to different temperatures. The FTIR spectrum of cross-linked PCS heated to 500°C is essentially similar to that of cross-linked PCS, but there is a decrease in intensity of absorption of all the peaks. There is a marked change in the spectrum upon heating the PCS to 650°C, as seen by the 30% weight loss. The 2950 cm⁻¹ and the 2895 cm⁻¹ peaks are almost removed, as is the 2100 cm⁻¹ peak. The two prominent peaks are those at 1015 cm⁻¹ (CH₂-wagging) and at 815 cm⁻¹ (Si-C stretching). The 1015 cm⁻¹ peak disappears upon heating the PCS to 800°C and a new peak appears at 1090 cm⁻¹ (due to Si-O stretching).

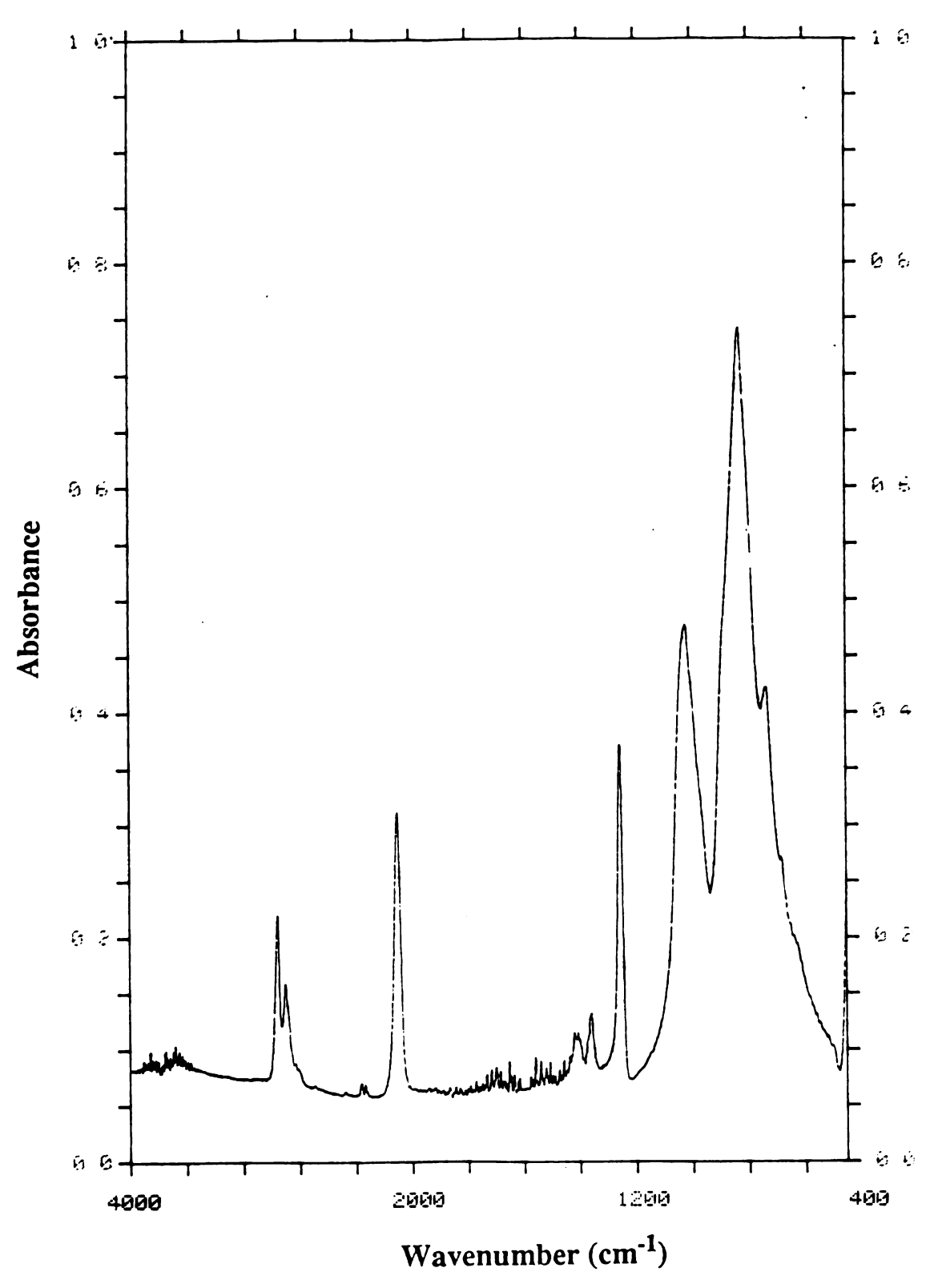


Figure 14. FTIR spectrum of cross-linked polycarbosilane (PCS)

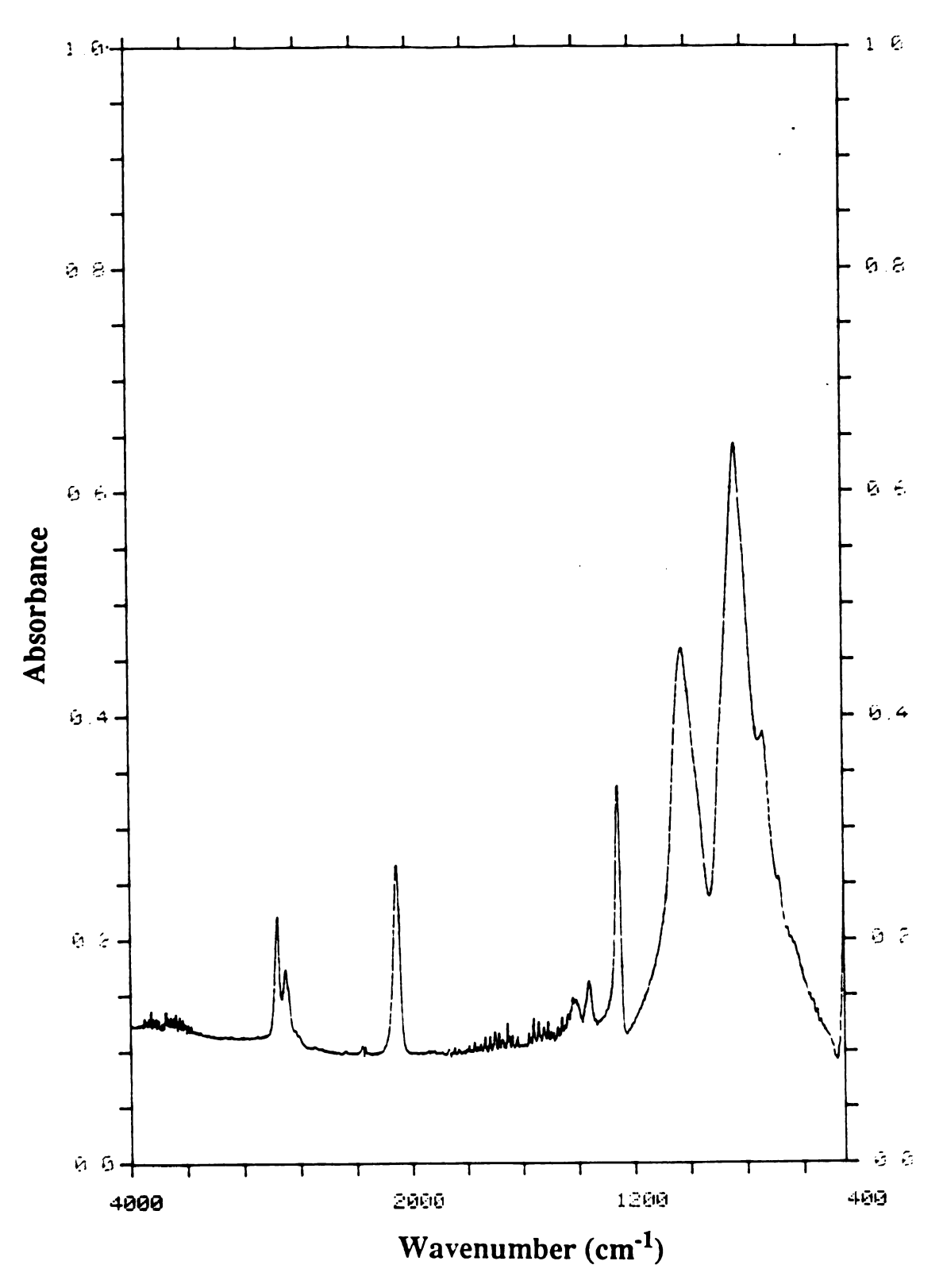


Figure 15. FTIR spectrum of cross-linked PCS heated to 500°C

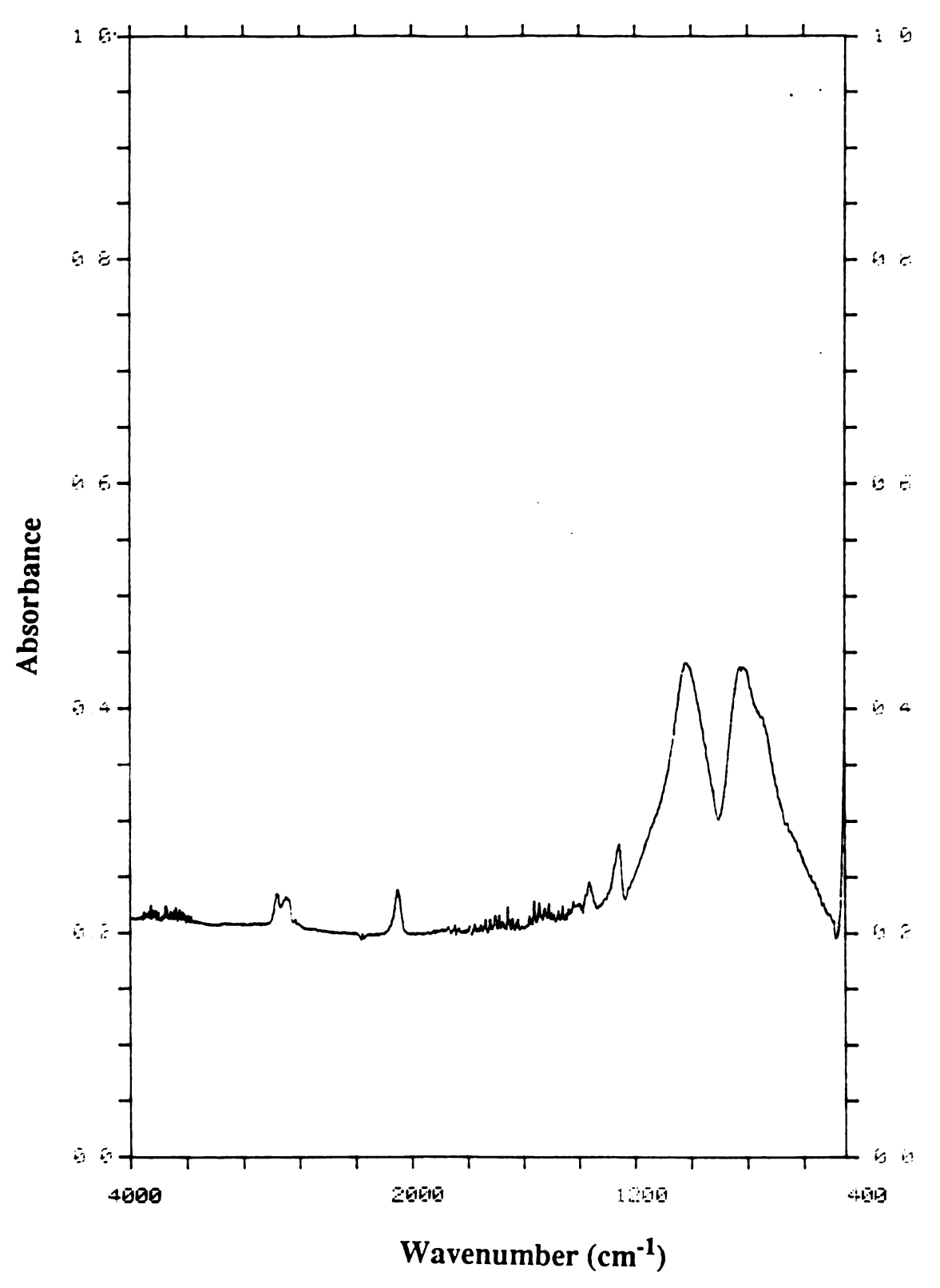


Figure 16. FTIR spectrum of cross-linked PCS heated to 650°C

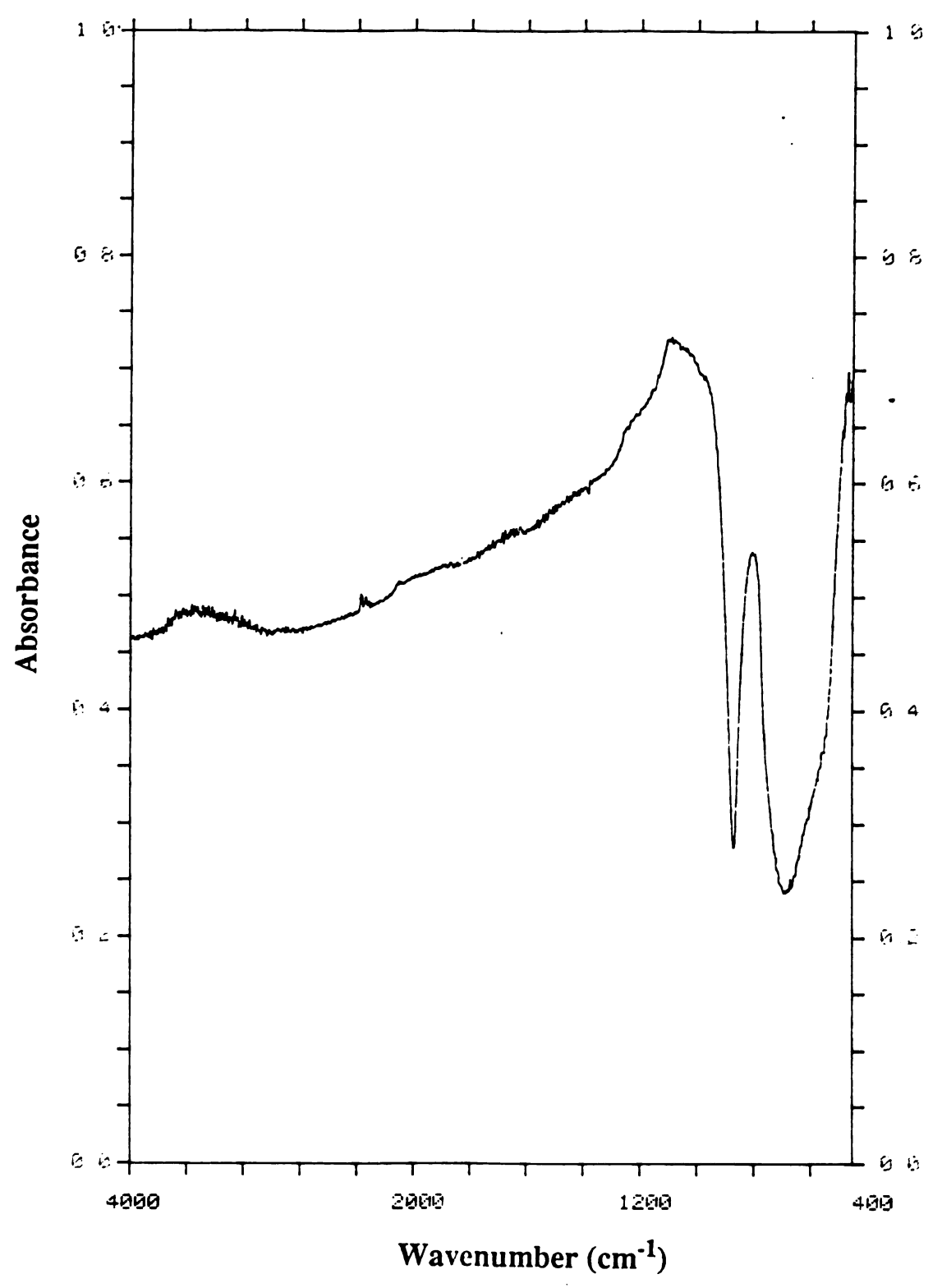


Figure 17. FTIR spectrum of cross-linked PCS heated to 800° C

3.2. RESULTS OF PRE-DENSIFICATION OF SILICA AEROGELS

The objective of the pre-densification step was to obtain silica aerogels with a density of 1.00 g/cc. The value of 1.00 g/cc was chosen as the desired gel density that could withstand the infiltration of PCS. It was observed that the densification behaviour of silica aerogels upon thermal treatment depended on the time between the end of the drying step and the start of the thermal treatment step (storage time). The actual temperature of pre-densification that was needed to obtain gels of 1.00 g/cc density was dependent on this storage time. Other factors that affect the density of the pre-densified aerogel are anneal temperature and the time of dwell at the anneal temperature (hold time).

The effect of hold time on the final density of silica aerogel is shown in Table 3. Aerogels that had been stored for a period of 3-7 days and annealed at 1050°C reached a density of 1.00 g/cc after a 12 hour hold time. Increasing the hold time longer than 12 hours did not alter the density of the aerogel. Table 4 shows the variation of density with the storage time for a given anneal temperature (1050°C) and holding time (12 hours). The density of silica aerogel increases with increasing storage time. Table 5 shows the densification behaviour of aerogels that have been stored for a given time (0-3 days), upon annealing at different temperatures (constant hold time of 12 hours). As can be expected, higher anneal temperatures resulted in aerogels with

Table 3. Variation of density of silica aerogel with hold time

Storage time (days)	Temp. of pre-dens. (°C)	Hold time (hrs.)	Density (g/cc)
3-7	1050	15	1.00
3-7	1050	12	1.00
3-7	1050	8	0.80
3-7	1050	6	0.75
3-7	1050	0.5	0.60

Table 4. Variation of density of silica aerogel with storage time

Storage time (days)	Anneal temperature (°C)	Hold time (hrs.)	Density (g/cc)
0-3	1050	12	0.80
3-7	1050	12	1.00
7-14	1050	12	1.10
14-28	1050	12	1.40

Table 5. Variation of density of silica aerogel with temperature

Anneal temperature (°C)	Storage time (days)	Hold time (hrs.)	Density (g/cc)
1075	0-3	12	1.10
1050	0-3	12	0.80
1025	0-3	12	0.70
1000	0-3	12	0.65

higher densities.

The dependence of the densification of silica aerogels on the storage time has not been reported elsewhere. The adsorption of moisture by the aerogels upon storage is a probable cause for altering the densification behaviour. The [OH] content in a silicate gel has been shown to affect the viscosity of the gel ⁶⁴. Increased [OH] content leads to reduced viscosity, thereby resulting in a lower densification temperature or a greater extent of densification at a given temperature. Structural relaxation of the aerogel with time ⁶³ is also a factor that can affect the densification of aerogels.

Pre-densification of bars resulted in some warping and bending, probably due to uneven heating. To avoid warpage problems, bars were loaded in the furnace with a weight on top, as described in section 2.3 (Chapter 2).

3.3. RESULTS OF POLYCARBOSILANE INFILTRATION

The extent of infiltration of PCS into the matrix of the pre-densified silica aerogel depended primarily on the density of the aerogel after pre-densification. The results of PCS infiltration into the aerogel matrix of small bars are summarized in Table 6. For a PCS solution of a given concentration in hexane, the lower the density of the aerogel, the higher the PCS concentration in the infiltrated aerogel. However, an aerogel of too low a density cracks upon removal out of the PCS solution, due to surface tension forces set up by the evaporating hexane.

Table 6. Polycarbosilane infiltration data

Density of pre- dens. aerogel (g/cc)	Weight% PCS in hexane	Weight% PCS in infilt. aerogel	Theo. SiC load. in composite (wt%)	
0.70	30	15	11	
0.70	25	12	10	
0.70	20	10	8	
0.70	10	5	3.5	
0.80	30	10	8	
0.80	20	7	5.5	
0.80	10	3	2	
0.90	40	10	8	
0.90	20	5	3.5	
0.90	10	2	1.5	
1.00	30	6	4.5	
1.10	30	3	2	
1.10	10	1	0.7	

Too high a density of the aerogel prevents cracking but limits the amount of PCS that can be incorporated in the aerogel matrix. Predensified gels with densities as low as 0.60 g/cc were used in the infiltration step. However, the lower limit of density which resulted in crack-free infiltrated gels was 0.80 g/cc. A safe and reasonable value of 1.00g/cc was hence chosen as the desired density in the pre-densification step.

Determination of the final composite composition (wt% SiC) was done in the following way. Considering 1 gram of the infiltrated aerogel as the basis, let "x" be equal to the weight(g) of PCS in the infiltrated aerogel. Then the weight(g) of predensified silica in the infiltrated aerogel is equal to "1-x". Upon pyrolysis and densification, SiC is formed with a 68% weight loss and dense silica is formed with a 2.5% weight loss in the composite. Therefore, weight(g) of SiC in the composite equals 0.68x and the weight(g) of SiO₂ equals 0.975(1-x). So, the weight% SiC in the composite is given by the following relation:

%SiC(wt) in composite=0.68x/(0.975-0.295x)

3.4. RESULTS OF CROSS-LINKING OF POLYCARBOSILANE

Polycarbosilane needs to be cross-linked before it is converted to SiC. Oxygen cross-linking, as described by Yajima, was used to cross-link the PCS. This is primarily an oxidation reaction that is accomplished by slow heating to a temperature in the 200-250°C range. A typical reaction that takes place during

cross-linking is shown below. The Si-H bond of the PCS structure reacts with oxygen to form the Si-O-Si unit.

$$- Si - H + - Si - H + O_2$$
 $- Si - O - Si - + H_2O$

The formation of Si-O-Si network results in a weight gain of the PCS after cross-linking. If w_1 is the weight(g) of PCS before cross-linking and w_2 is the weight(g) of PCS after cross-linking, Ichikawa et al.⁶⁵ defined $\Delta w/w = (w_2-w_1)/w_1$. They subsequently conducted strength testing, modulus measurements, and XRD analysis on SiC produced using PCS samples cross-linked to different $\Delta w/w\%$. It was observed that SiC produced with PCS samples cross-linked to a $\Delta w/w\%$ of $\sim 8\%$ showed the best properties. Excessive cross-linking introduced a high content of Si-O bonds in the polymeric network, thereby affecting the properties of SiC.

The cross-linking conditions that result in different $\Delta w\%$ for PCS infiltrated into silica aerogel matrices are shown in Table 7.

3.5. RESULTS OF THE PYROLYSIS OF POLYCARBOSILANE AND DENSIFICATION OF SILICA

Figure 18 shows the change in density of both the silica aerogel and the SiO_2/SiC composite as a function of anneal temperature. Silica aerogel attained a density of 2.2 g/cc at

Table 7. Conditions for cross-linking of polycarbosilane infiltrated in silica aerogel matrix

Temperature (°C)	Hold time (min.)	Δw %	
210	30	2	
220	30	3	
230	30	6	
240	30	8	
260	30	8	

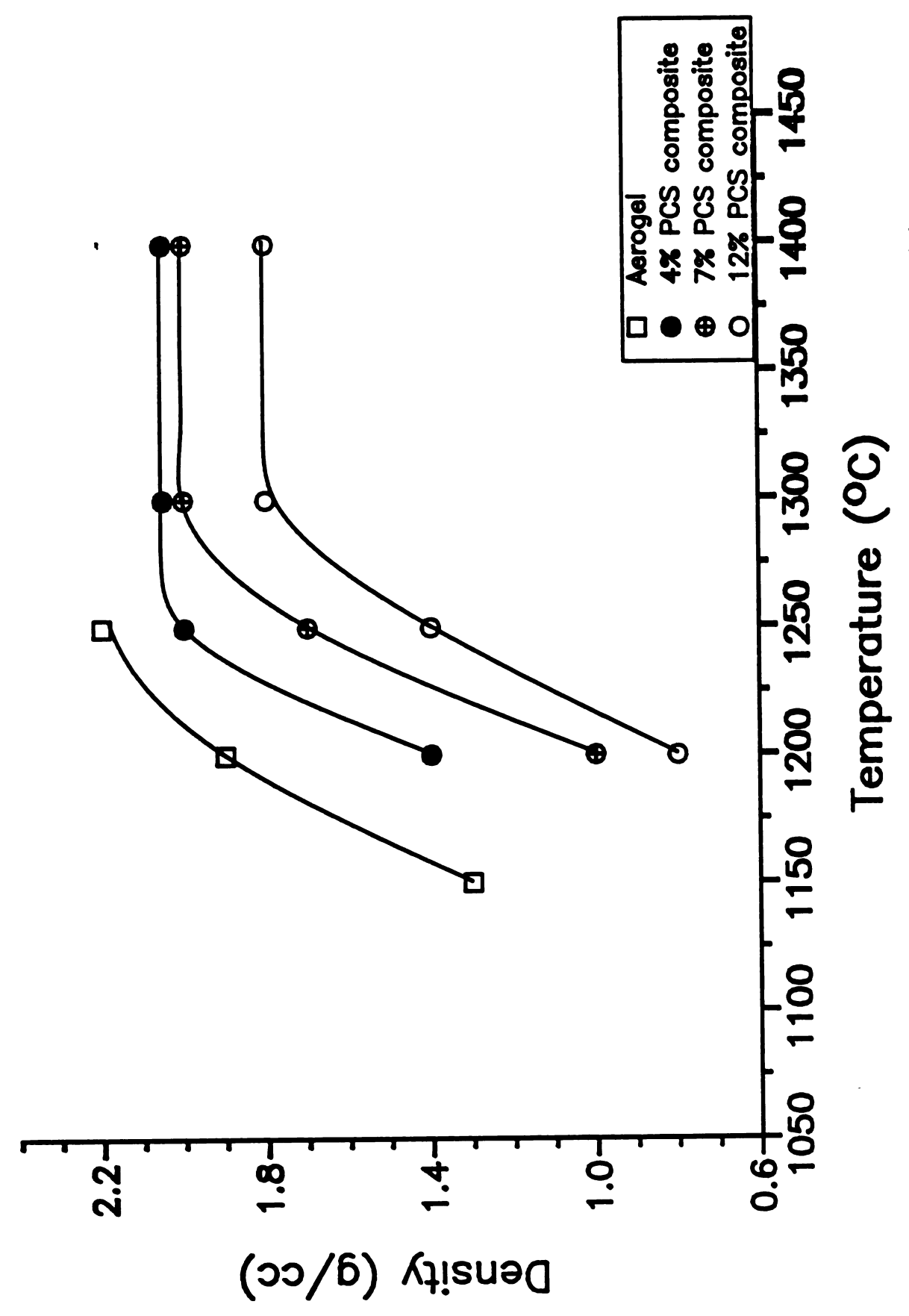


Figure 18. Variation of density of processed specimens with anneal temperature

1250°C. There is a sharp increase in density as the anneal temperature is increased in the 1100-1250°C range. Upon heating to temperatures greater than 1250°C, bloating of the gels occurred.

The densification behaviour of the composite is similar, but is shifted to higher temperatures. The SiO₂/SiC composite with 4% PCS by weight reached a density of 2.05-2.10 g/cc at 1300°C. The 7% PCS (wt%) composite had a density of 2.00 g/cc at 1300°C and the 12% PCS(wt%) composite had a density of 1.80 g/cc. The presence of the SiC phase in the matrix inhibits complete densification of the composite.

SiO₂/SiC composites containing greater than 12% PCS by weight could not be processed since the specimens were extensively cracked on a macroscopic scale. This lack of monolithicity at higher PCS loadings is attributed to the following reasons:

- 1. Evolution of gases upon pyrolysis of PCS causes flaws and pores and leads to disruption of the mechanical integrity of the weak gel structure
- 2. Thermal expansion and modulus mismatches between silica and silicon carbide become more significant.

The FTIR spectrum of SiO₂/SiC composite is shown in Figure 19. The spectrum has three characteristic peaks; the peak

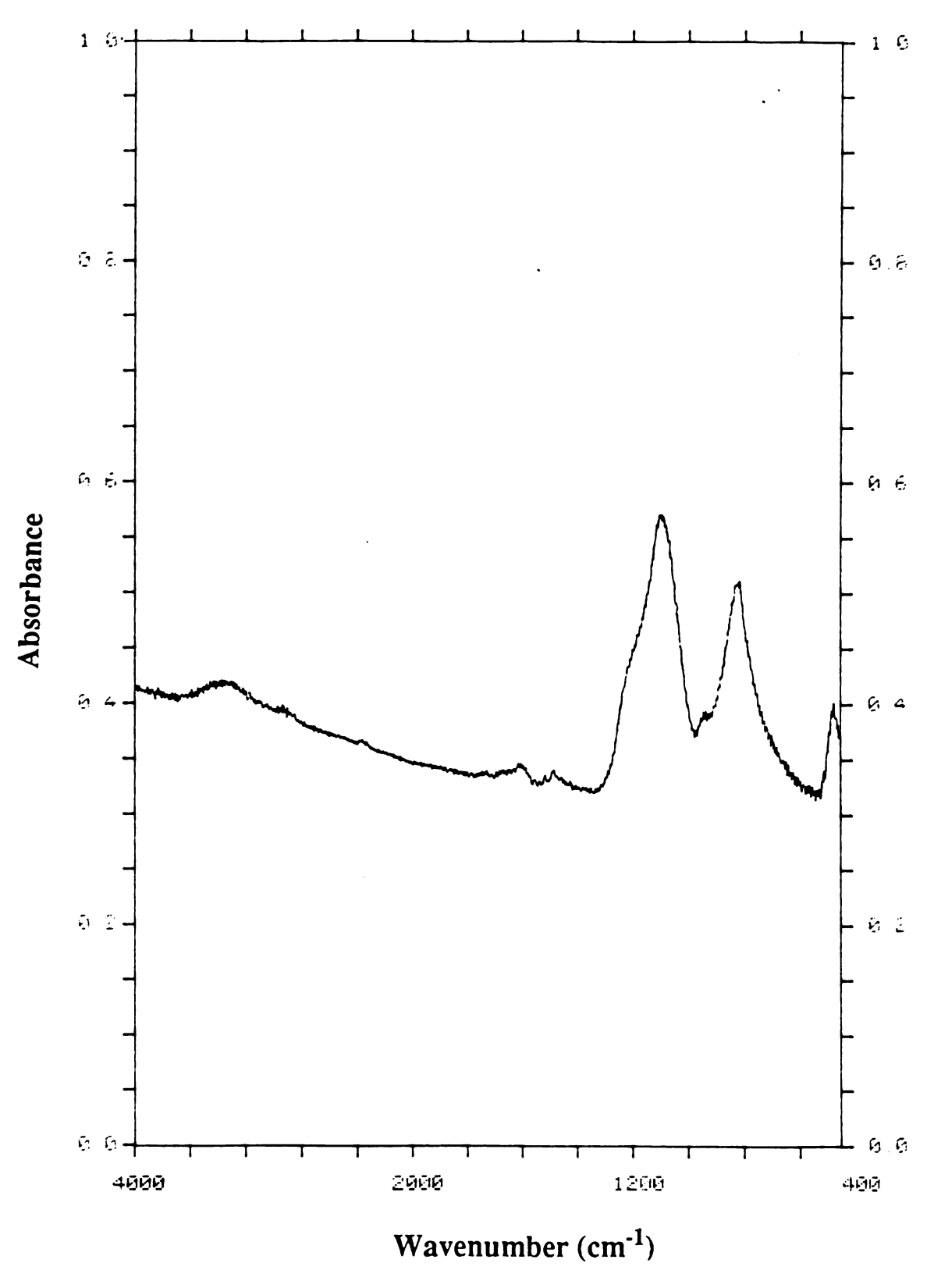


Figure 19. FTIR spectrum of SiO₂/SiC composite

at 1090 cm⁻¹ is due to Si-O stretching, the peak at 815 cm⁻¹ is due to Si-C stretching, and the peak at 470 cm⁻¹ corresponds to Si-O-Si-O deformation. Figure 20 is a photograph of some of the processed specimens. A silica aerogel bar with a density of 0.2 g/cc is shown on the top. The middle specimen is dense silica (density of 2.2 g/cc) and the specimen in the bottom is SiO₂/SiC composite of density 2.0 g/cc.

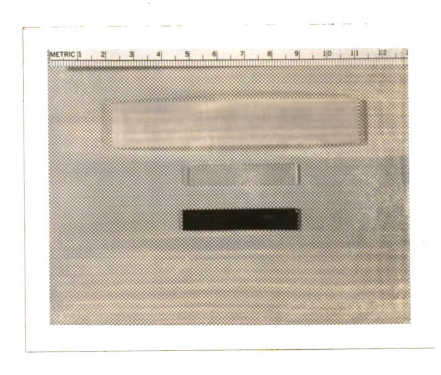


Figure 20. Photograph of processed specimens: top-silica aerogel, middle-densified silica, and bottom-SiO₂/SiC composite

Chapter 4

CONCLUSIONS AND RECOMMENDATIONS

The steps involved in the overall processing of the silca/silicon carbide composite are outlined below:

- (i) conversion of silica sols to gels and drying the gels using supercritical CO_2 to obtain silica aerogels with a density of 0.2 g/cc
- (ii) pre-densification of silica aerogels by a thermal treatment step to obtain gels with a density of 1.00 g/cc
- (iii)infiltration of a solution of polycarbosilane in hexane, into the matrix of the pre-densified

aerogel

(iv) simultaneous pyrolysis of polycarbosilane (to form SiC) and densification of the silica matrix, via a high temperature anneal, to form the composite.

SiO₂/SiC composite specimens of different geometries, containing polycarbosilane up to 12 weight% (after infiltration), were produced. The densities of the composite specimens ranged from 1.8 g/cc (12 wt% PCS) to 2.05 g/cc (4 wt% PCS). The density of silica specimens was 2.2 g/cc. It was not possible to fabricate composite specimens containing greater than 12 wt% PCS because the specimen was cracked extensively and did not retain its monolithic structure.

Microhardness of the composite was measured as a function of the PCS content by Mr. C.-C. Chiu and was observed to be higher than that of silica. A maximum hardness of 8.7 GPa was obtained with the composite containing 7 wt% PCS after infiltration, compared to a value of 5.8 GPa for monolithic silica, under an indentation load of 9.8 N.

The potential advantages of the process include:

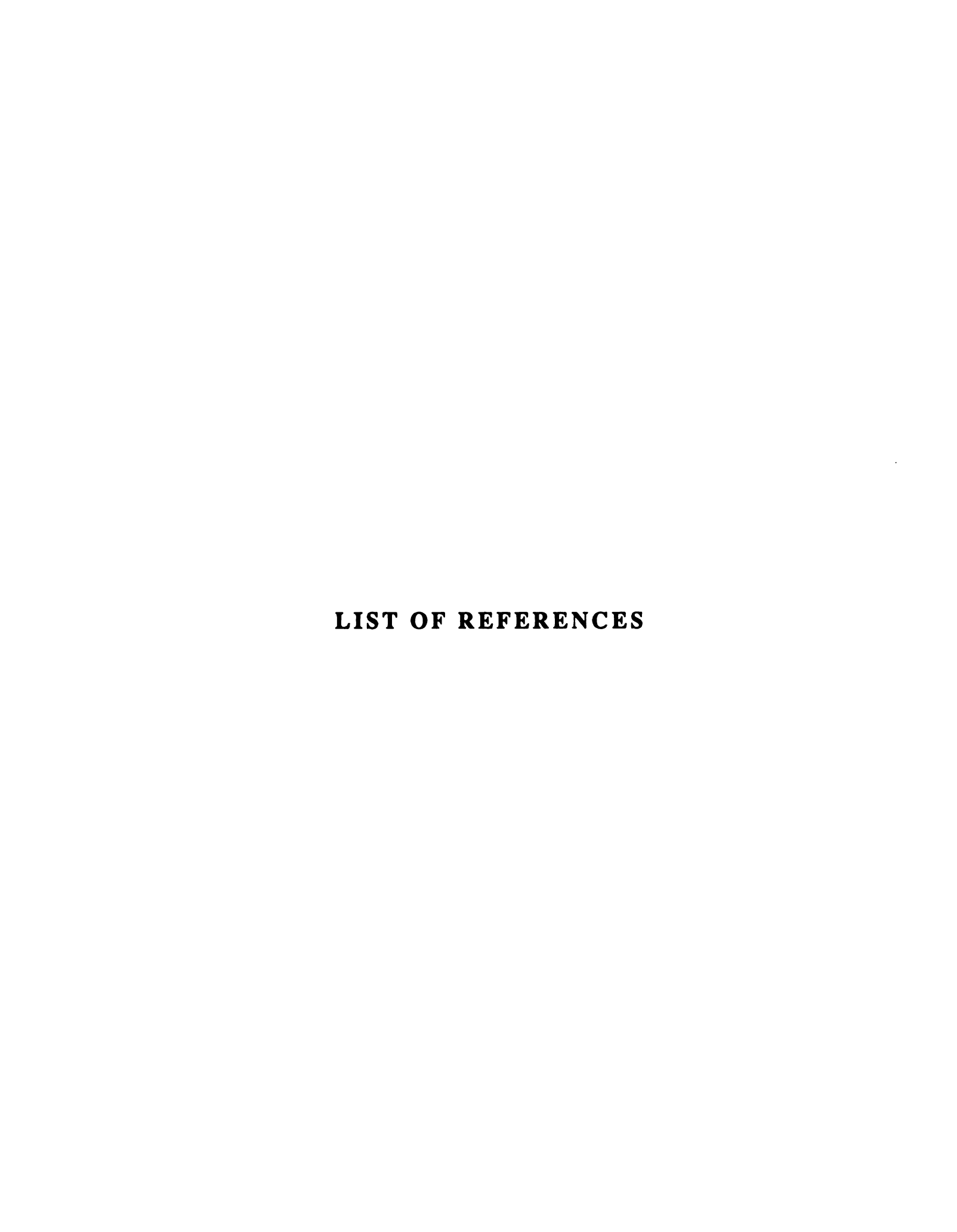
- a) low temperature fabrication due to the sol-gel approach
- b) easy moldability of different geometries
- c) no complex processing equipment is required.

The disadvantages of the processing method are:

a) high shrinkage

b) limitation on the amount of polycarbosilane that can be infiltrated into the matrix.

multiple processing steps involved the composite fabrication need to be better understood. The infiltration process has been studied on the basis of the specimen bulk density. The relationship between the pore distribution in the aerogel and the infiltration conditions needs to be established. Another factor that needs to be studied is the effect of crosslinking of PCS on the properties of the composite. At this point there is no clear evidence of the nature of the reinforcing phase, SiC. Is it present in the matrix in some fibrillar form? If so, is it possible to alter the composite properties by tailoring the pore size distribution in the aerogel, thereby changing the fibril geometry? The design of the furnace seal for inert gas connections must be modified to enable better gas purge. The fabrication process that has been developed can be extended to other matrices and reinforcements.



LIST OF REFERENCES

- 1. Mehrotra, R.C., J. Non. Cryst. Solids, 100, 1, (1988).
- 2. Hubert-Pfalzgraf, L.G., New. J. Chem., 11, 663, (1987).
- 3. Yoldas, B.E., J. Non. Cryst. Solids, 82, 11, (1986).
- 4. Yoldas, B.E., J. Non. Cryst. Solids, 83, 375, (1986).
- 5. Hasegawa, I., Sakka, S., J. Non. Cryst. Solids, 100, 201, (1988).
- 6. Pope, E.J.A., Mackenzie, J.D., J. Non. Cryst. Solids, 87, 185, (1986).
- 7. Sakka, S., Kamiya, K., J. Non. Cryst. Solids, 48, 31, (1982).
- 8. Pouxviel, J.C., Boilot, J.P., Beloeil, J.C., Lallemand, J.Y., J. Non. Cryst. Solids, 89, 345, (1987).
- 9. Kistler, S.S., Nature, 127, 741, (1931).
- 10. Peri, A.B., J. Phys. Chem., 70, 2937, (1966).
- 11. Teichner, S.J., Nicolaon, G.A., Vicarini, M.A., Gardes, G.E.E., Adv. Colloid Interface Sci., 5, 245, (1976).
- 12. Zarzycki, J., Prassas, M., Phalippou, J., J. Mat. Sci., 19, 1656, (1984).
- 13. Tewari, P.H., Hunt, A.J., Lofftus, K.D., Mat. Lett., 3, 363, (1985)
- 14. Rangarajan, B., Lira C.T., submitted to J. Supercritical Fluids.
- 15. Decottignies, M., Phalippou, J., Zarzycki, J., J. Mat. Sci., 13, 2605, (1978).
- 16. Yamane, M., Aso, S., Okano, S., Sakaino, T., J. Mat. Sci., 14, 607, (1979).

- 17. Prassas, M., Phalippou, J., Zarzycki, J., Science of Ceramic Chemical Processing, edited by L.L. Hench and D.R. Ulrich, John Wiley, 156, (1986).
- 18. Bertoluzza, A., Fagnano, C., Morelli, M.A., Gottardi, V., Gaglielmi, M., J. Non. Cryst. Solids, 48, 117, (1982).
- 19. Phalippou, J., Woignier, T., Zarzycki, J., Ultrastructure processing of ceramics, glasses, and composites, edited by L.L. Hench and D.R. Ulrich, Wiley, 70, (1984).
- 20. Rabinovich, E.M., Wood, D.L., Johnson Jr., D.W., Fleming, D.A., Vincent, S.M., MacChesney, J.B., J. Non. Cryst. Solids, 82, 42, (1986).
- 21. Brinker, C.J., Scherer, G.W., J. Non. Cryst. Solids, 70, 301, (1985).
- 22. Chantrell. P.G., Popper, P., Special Ceramics 1964, edited by P. Popper, Academic Press, 87, (1965).
- 23. Yajima, S., Okamura, K., Hayashi, J., Omori, M., J. Am. Ceram. Soc., 59, 324, (1976).
- 24. Yajima, S., Hasegawa, Y., Hayashi, J., Iimura, M., J. Mat. Sci., 13, 2659, (1978).
- 25. Hasegawa, Y., Iimura, M., Yajima, S., J. Mat. Sci., 15, 720, (1980).
- 26. Hasegawa, Y., Okamura, K., J. Mat. Sci., 18, 3633, (1983).
- 27. West, R., David, L.D., Djurovich, P.I., Stearley, K.L., Srinivasan, K.S.V., Yu, H., J. Am. Chem. Soc., 103, 7352, (1981).
- 28. West, R., David, L.D., Djurovich, P.I., Am. Cerm. Soc. Bull., 62, 899, (1983).

- 29. West, R., Zhang, X-H., Djurovich, P.I., Stuger, H., Science of Ceramic Chemical Processing, edited by L.L. Hench and D.R. Ulrich, John Wiley, 337, (1986).
- 30. Lee, B.I., Hench, L.L., Science of Ceramic Chemical Processing, edited by L.L. Hench and D.R. Ulrich, John Wiley, 345, (1986).
- 31. Lenz, R.W., Dvornic, P.R., Polymer, 24, 763, (1983).
- 32. Schilling Jr., C.L., British Polymer Journal, 18, 355, (1986).
- 33. Gaul, Jr., J.H., US Pat. 4,340,619, (July 1982).
- 34. Gaul, Jr., J.H., US Pat. 4,395,460, (July 1983).
- 35. Seyferth, D., Wiseman, G.H., Science of Ceramic Chemical Processing, edited by L.L.Hench and D.R. Ulrich, John Wiley, 354, (1986).
- 36. Laine, R.M., Blum, Y.D., Hamlin, R.D., Chow, A., Ultrastructure Processing of Advanced Ceramics, edited by J.D. Mackenzie and D.R. Ulrich, John Wiley, 761, (1988).
- 37. Paciorek, K.J.L., Harris, D.H., Krone-Schmidt, W., Kratzer, R.H., Ultrastructure Processing of Advanced Ceramics, edited by J.D. Mackenzie and D.R. Ulrich, John Wiley, 89, (1988)
- 38. Seibold, M., Russel, C., Better Ceramics through Chemistry III, edited by C.J. Brinker, D.E. Clark, and D.R. Ulrich, Materials Research Society, 477, (1988).
- 39. Claussen, N., J. Am. Ceram. Soc., 59, 49, (1976).
- 40. Lange, F.F., J. Mater. Sci., 17, 247, (1982).
- 41. Wei, G.C., Becher, P.F., J. Am. Ceram. Soc., 67, 571, (1984).
- 42. Wahi, R.P., Ilschner, B., J. Mater. Sci., 15, 875, (1980).

- 43. Mah, T.I., Mendiratta, M.G., Lipsitt, H., Am. Ceram. Soc. Bull., 60, 1229, (1981).
- 44. Dutta, S., Buzek, B., J. Am. Ceram. Soc., 67, 89, (1984).45.
 Mah, T.I., Mendiratta, M.G., Katz, A.P., Mazdiyasni, K.S., Am.
 Cerm. Soc. Bull., 66, 304, (1987).
- 46 Buljan, S.T., Baldoni, J.G., Huckabee, M.L., Am. Ceram. Soc. Bull., 66, 347, (1987).
- 47. Shalek, P.D., Petrovic, J.J., Hurley, G.F., Gac, F.D., Am. Ceram. Soc. Bull., 65, 351, (1986).
- 48. Gadkaree, K.P., Chyung, K., Am. Ceram. Soc. Bull., 65, 370, (1986).
- 49. Wei, G.C., Becher, P.F., Am. Ceram. Soc. Bull., 64, 298,(1985).
- 50. Prewo, K.M., Brennan, J.J., Layden, G.K., Am. Ceram. Soc. Bull., 65, 305, 322, (1986).
- 51. Lamicq, P.J., Bernhart, G.A., Dauchier, M.M., Mace, J.G., Am. Ceram. Soc. Bull., 65, 336, (1986).
- 52. Caputo, A.J., Lackey, W.J., Stinton, D.P., Ceram. Eng. Sci. Proc., 6, 694, (1985).
- 53. Rice, R.W., Ceram. Eng. Sci. Proc., 2, 661, (1981).
- 54. Hillig, W.B., Ceram. Eng. Sci. Proc., 6, 674, (1985).
- 55. Stinton, D.P., Caputo, A.J., Lowden, R.A., Am. Ceram. Soc. Bull., 65, 347, (1986).
- 56. Lannutti, J.J., Clark, D.E., Better Ceramics through Chemistry, edited by C.J. Brinker, D.E. Clark, and D.R. Ulrich, North Holland, 369, (1984).

- 57. Lannutti, J.J., Clark, D.E., Better Ceramics through Chemistry, edited by C.J. Brinker, D.E. Clark, and D.R. Ulrich, North Holland, 375, (1984).
- 58. Lee, B.I., Hench, L.L., Science of Ceramic Chemical Processing, edited by L.L. Hench and D.R. Ulrich, John Wiley, 231, (1986).
- 59. Lee, B.I., Hench, L.L., Ceramic Eng. Sci. Proc., 7, 994, (1986).
- 60. Qi, D., Pantano, C.G., Ultrastructure Processing of Advanced Ceramics, edited by J.D. Mackenzie and D.R. Ulrich, 635, (1988).
- 61. Park S.Y., Lee, B.I., J. Non. Cryst. Solids, 100, 345, (1988).
- 62. Fricke, J., Reichenauer, G., J. Non. Cryst. Solids, 95 & 96, 1135, (1987).
- 63. Mohanakrishnan, C.K., Rangarajan, B., Miller, D.J., Lira, C.T., Chiu, C.-C., Case, E., 5th Technical Conference on Composite Materials, ASC, 882, (1990).
- 64. Brinker, C.J., Roth, E.P., Tallant, D.R., Scherer, G.W., Science of Ceramic Chemical Processing, edited by L.L. Hench and D.R. Ulrich, John Wiley, 37, (1986).
- 65. Ichikawa, H., Teranishi, H., Ishikawa, T., J. Mat. Sci. lett., 6, 420, (1987).

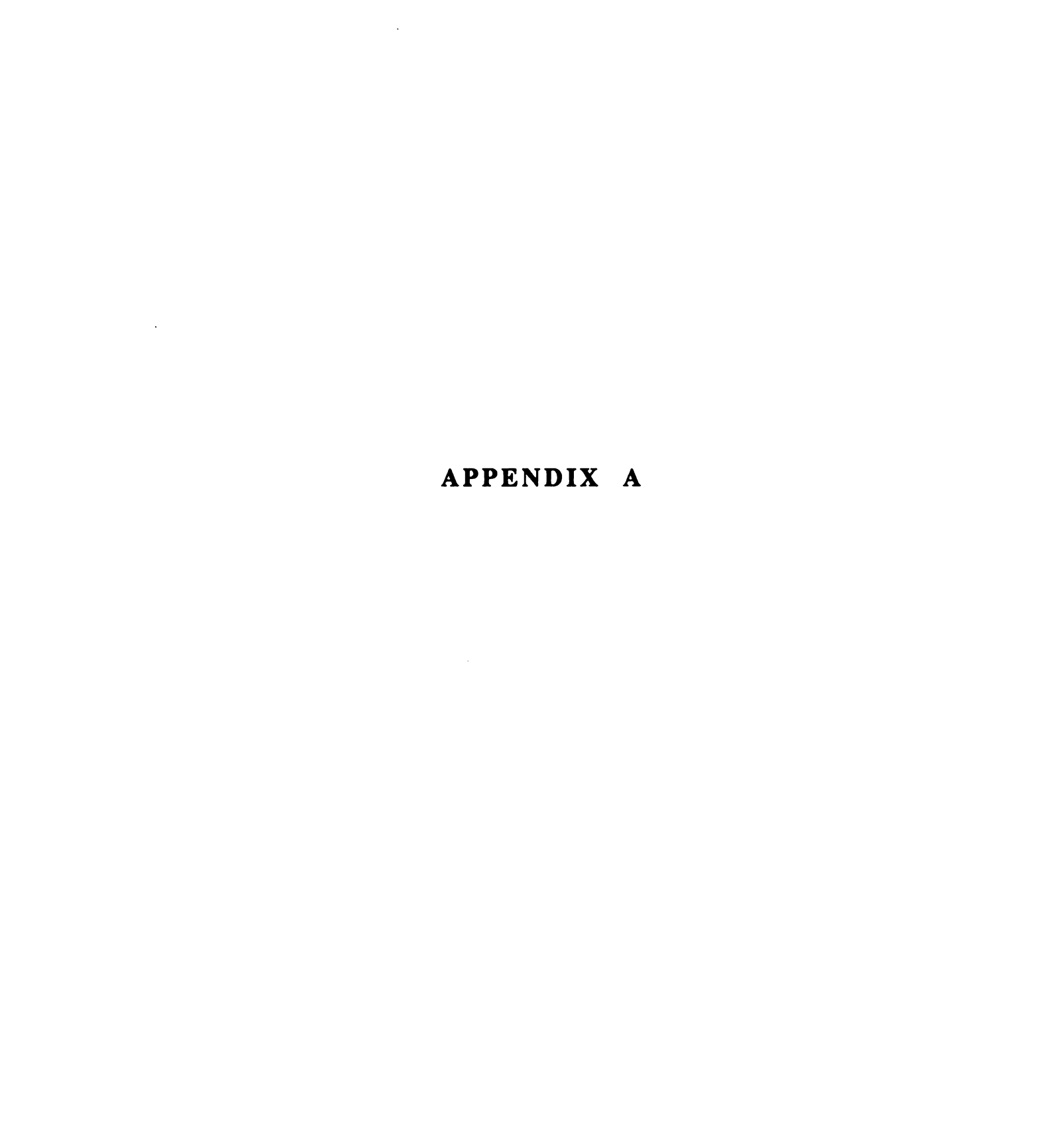


Table A1. Pore size distribution of silica aerogel by mercury porosimetry

MICROMERITICS PORE SIZER 9310

GEL 25 MOHANAKRISHNAN C.K. PENETROMETER NUMBER 161

1/11/88 2.30 PM

PRESSURE FSIA	CORRECTED PRESSURE PSIA	PORE DIAMETER um	CUM. INTR. VOLUME CC/g	CUM. FORE SURFACE AREA m2/g	DIFF. INTR. VOLUME dV&dD cc/g um	INCR. INTR. VOLUME cc/g
2.1	2.1	86.6199	0.0000	0.0000	0.0000	0.0000
3.9	3.9	46.5181	0.0120	0.0007	0.0003	0.0000
5.0	5.0	35.9496	0.0120	0.0007	0.0000	0.0000
7.0	7.0	25.7969	0.0120	0.0007	0.0000	0.0000
8.2	8.2	21.9867	0.0120	0.0007	0.0000	0.0000
10.1	10.1	17.8312	0.0120	0.0007	0.0000	0.0000
12.3	12.3	14.6578	0.0120	0.0022	0.0000	0.0060
14.2	14.2	12.7108	0.0300	0.0022	0.0014	0.0020
		11.0174	0.0300	0.0057	0.0000	0.0000
16.4 18.2	16.4 18.2	9.9435	0.0300	0.0057	0.0000	0.0000
19.5	19.5	9.2736	0.0300	0.0057	0.0000	0.0000
21.3	21.3	8.4972	0.0300	0.0057	0.0000	0.0000
22.7	22.7	7.9777	0.0360	0.0037	0.0000	0.0060
25.0	29.6	6.1030	0.0360	0.0086	0.0000	0.0000
50.0	54.6	3.3131	0.0320	0.0392	0.0129	0.0360
100.0	104.5	1.7307	0.1440	0.1534	0.0129	0.0380
255.0	259.1	0.6981	0.4859	1.2797	0.3312	0.3420
499.0	502 .5	0.3599	0.9179	4.5459	1.2772	0.4320
7 5 3.0	756.2	0.2392	1.1999	8.3113	2.3357	0.4320
996.0	999.0	0.1810	1.3559	11.281	2.6832	0.1560
1504.0	1506.7	0.1200	1.5958	17.657	3.9336	0.2400
2488.0	2490.4	0.1200	1.8538	28.369	5.4408	0.2580
2992.0	2994.3	0.0604	1.9378	33.420	6.8722	0.0840
4008.0	4010.1	0.0451	2.0698	43.428	8.6258	0.1320
4976.0	4978.0	0.0363	2.1478	51.090	8.8936	0.1320
5984.0	5985.9	0.0302	2.2258	60.466	12.7488	0.0780
6968.0	6969 . 8	0.0302	2.2738	67.302	11.2520	0.0480
7968.0	7969.8	0.0227	2.3218	75.195	14.7415	0.0480
8992.0	8993.8	0.0201	2.3457	79.680	9.2879	0.0240
10000.0	10001.7	0.0181	2.3757	85.964	14.8012	0.0300
11944.0	11945.7	0.0151	2.4297	98.965	18.3486	0.0540
13936.0	13937.6	0.0130	2.4777	112.62	22.1804	0.0480
14944.0	14945.6	0.0121	2.4957	118.36	20.5648	0.0180
15920.0	15921.5	0.0114	2.5197	126.55	32.3504	0.0240
17768.0	17969.5	0.0101	2.5497	137.75	23.1699	0.0300
19928.0	19929.5	0.0091	2.5737	147.78	24.2438	0.0240
21912.0	21913.4	0.0083	2.6037	161.62	36.5091	0.0300
23888.0	23889.4	0.0076	2.6277	173.76	35.1520	0.0240
25880.0	25881.4	0.0070	2.6517	186.94	41.1836	0.0240
27864.0	27865.4	0.0065	2.6697	197.63	36.1740	0.0180
29854.0	29857.3	0.0061	2.6937	212.92	55.4175	0.0240

Table A1 (cont'd.).

MICROMERITICS PORE SIZER 9310

GEL 25 MOHANAKRISHNAN C.K. PENETROMETER NUMBER 161

1/11/88 2.30 FM

INCREMENTAL PORE VOLUME PER GRAM % vs. PORE DIAMETER (micrometers)

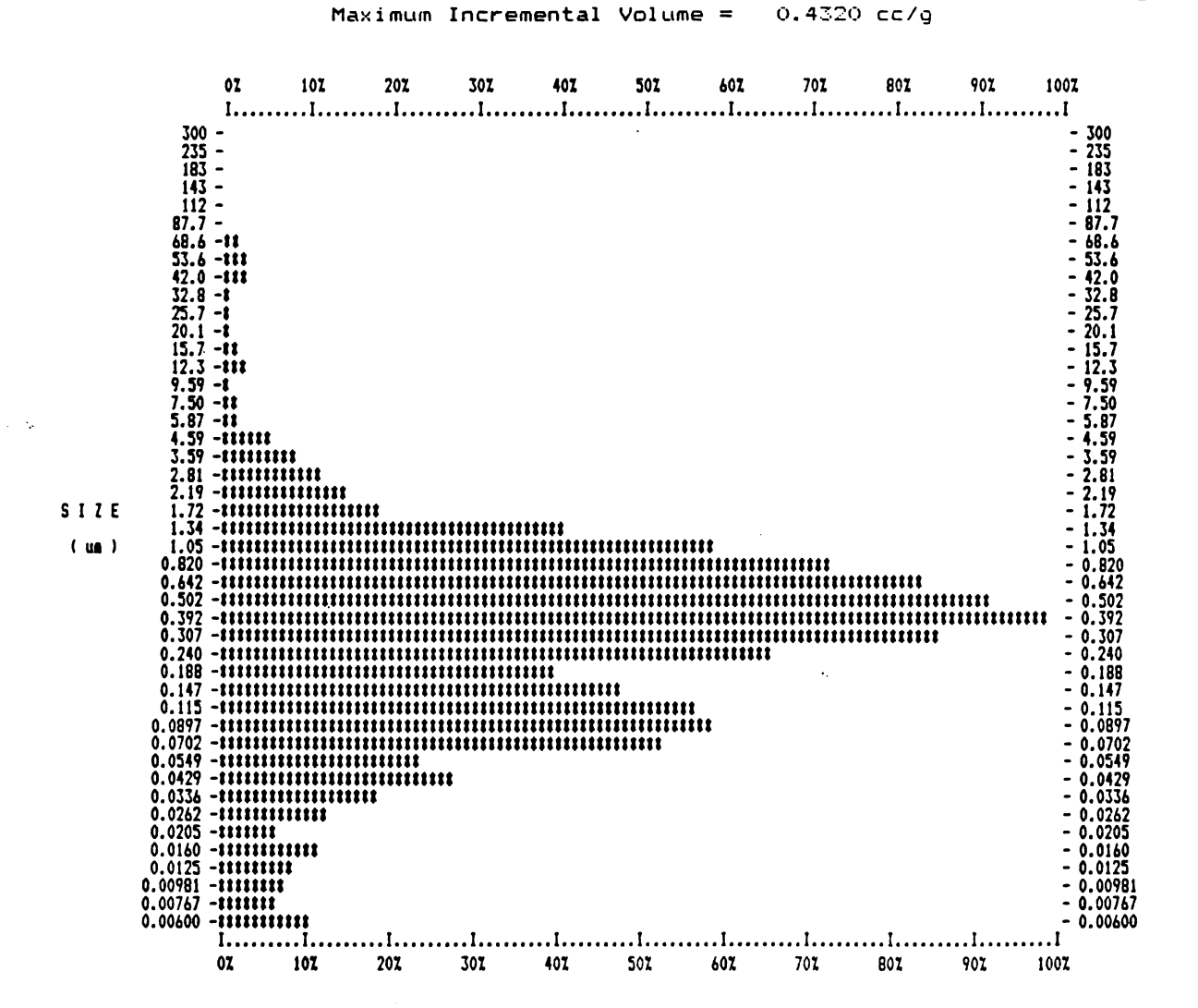


Table A1 (cont'd.).

MICROMERITICS PORE SIZER 9310

GEL 25 MOHANAKRISHNAN C.K. PENETROMETER NUMBER 161 1/11/88 2.30 FM

CUMULATIVE FORE VOLUME PER GRAM % vs. FORE DIAMETER (micrometers)
Maximum Intrusion = 2.6937 cc/g

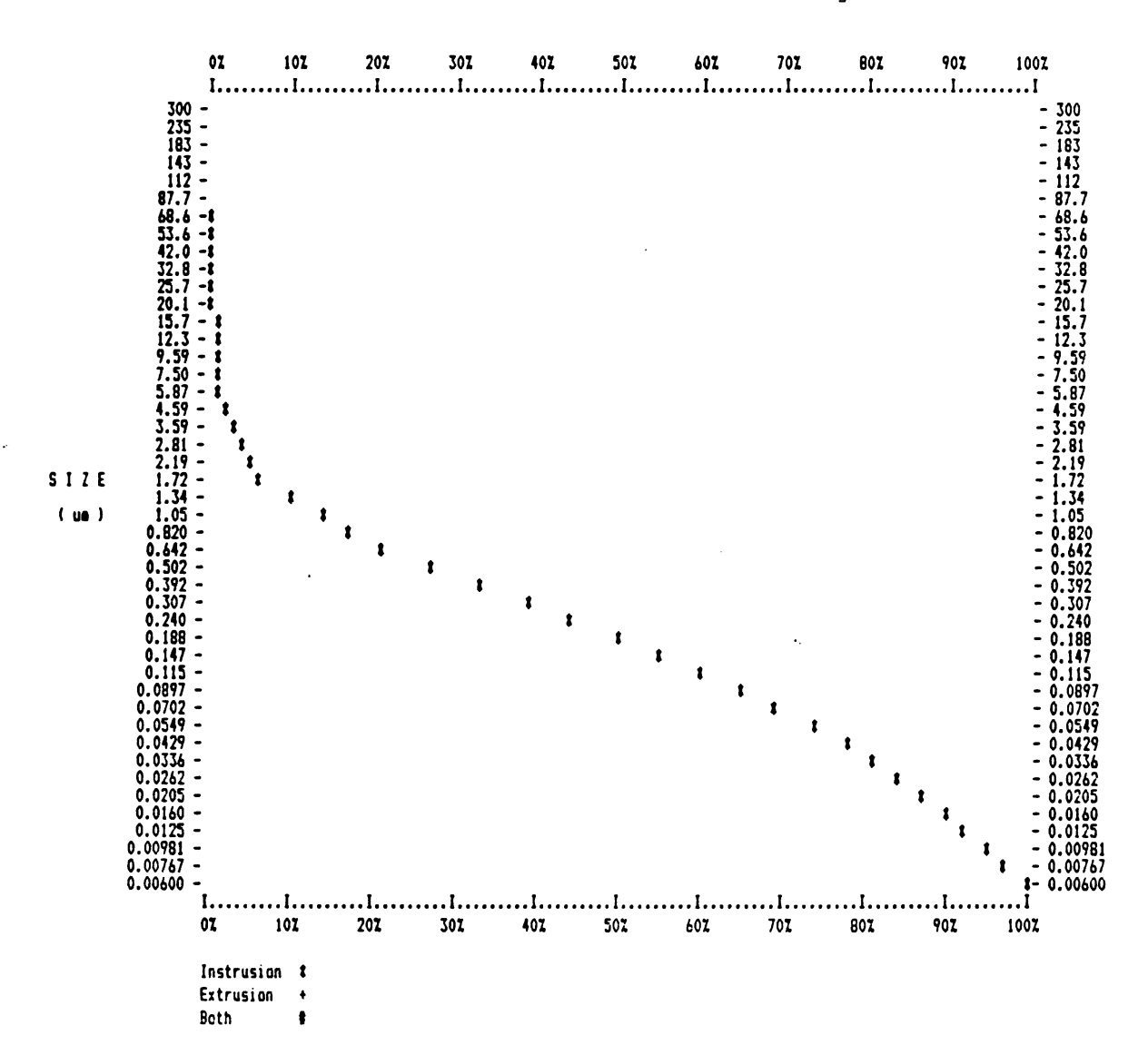
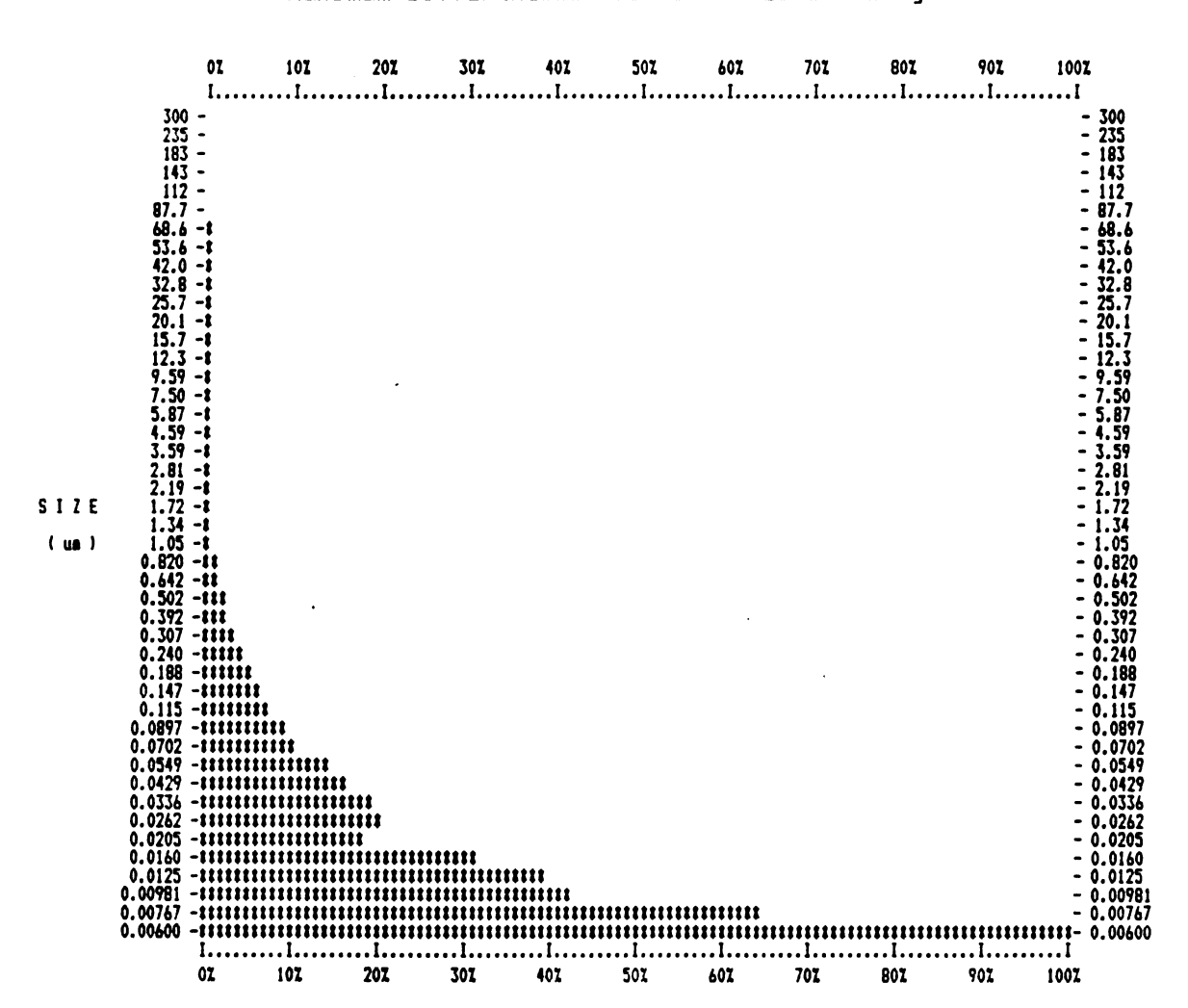


Table A1 (cont'd.).

MICROMERITICS PORE SIZER 9310

GEL 25 MOHANAKRISHNAN C.K. PENETROMETER NUMBER 161 1/11/88 2.30 PM

DIFFERENTIAL VOLUME PER GRAM % vs. PORE DIAMETER (micrometers)
Maximum Differential Volume = 55.4175 cc/g um



MICHIGAN STATE UNIV. LIBRARIES
31293008914271